

Received March 14, 2020, accepted March 26, 2020, date of publication March 30, 2020, date of current version April 24, 2020.

Digital Object Identifier 10.1109/ACCESS.2020.2984321

An Improved Grey Wolf Optimizer Based on Tracking and Seeking Modes to Solve Function Optimization Problems

M. W. GUO, J. S. WANG^{ID}, (Member, IEEE), L. F. ZHU, S. S. GUO^{ID}, AND W. XIE

School of Electronic and Information Engineering, University of Science and Technology Liaoning, Anshan 114051, China

Corresponding author: J. S. Wang (wang_jiesheng@126.com)

This work was supported in part by the Project by National Natural Science Foundation of China under Grant 21576127, in part by the Basic Scientific Research Project of Institution of Higher Learning of Liaoning Province under Grant 2017FWDF10, and in part by the Project by Liaoning Provincial Natural Science Foundation of China under Grant 20180550700.

ABSTRACT Grey wolf optimizer (GWO) is a new meta-heuristic algorithm. The GWO algorithm mimics the leadership hierarchy and hunting mechanism of grey wolves in nature. Three main stages of hunting include: encircling, tracking and attacking. It is easy to fall into local optimum when used to optimize high-dimensional data, and there is imbalance between exploration and exploitation. An improved grey wolf optimizer based on tracking mode and seeking mode is proposed to improve the diversity of the population and the ability of the algorithm to balance exploration and exploitation. The algorithm is verified by simulation experiments in three parts. Firstly, the proposed grey wolf optimizer based on tracking mode (TGWO), the improved grey wolf optimizer based on seeking mode (SGWO), the improved grey wolf optimizer based on tracking and seeking mode (TSGWO), Grey Wolf Optimizer (GWO), Particle Swarm Optimization (PSO), Salp Swarm Algorithm (SSA), Sine Cosine Algorithm (SCA), Ant Lion Optimizer (ALO), Whale Optimization Algorithm (WOA) and Moth-flame Optimization (MFO) are adopted to optimize 21 typical benchmark functions respectively, and the obtained statistical simulation results are compared; Secondly, the improved algorithm proposed in this paper is compared with Binary Grey Wolf Optimizer (BGWO), Hybrid PSOGWO Optimization (PSOGWO) and GWO Algorithm Integrated with Cuckoo Search (GWOCS); Finally, it is applied to the lightest design engineering problem of pressure vessels. Simulation results show that the superior performance of the proposed algorithm for exploiting the optimum and it has advantages in terms of exploration. The improved grey wolf optimizer based on tracking mode and seeking mode can better solve function optimization and classical engineering problems with constraints. It was found the improved grey wolf optimizer based on tracking mode has the high precision and the characteristics of balanced exploration and exploitation.

INDEX TERMS Grey wolf optimizer, tracking mode, seeking mode, function optimization.

I. INTRODUCTION

There are more and more demands for solving various complexity problems. In recent years, the emergence of meta-heuristic algorithms for bionics has emerged in an endless stream, and there is a faster way to solve many complex optimization problems. This kind of meta-heuristic algorithm has become a research hot-spot in solving optimization problems in recent years [1]. The concept of bionic algorithm was first introduced in the genetic algorithm (GA) [2]. Since

The associate editor coordinating the review of this manuscript and approving it for publication was Shadi Alawneh^{ID}.

then, Popular algorithms in this field include: Particle Swarm Optimization (PSO) [3]–[5]. Artificial Bee Colony algorithm (ABC) [6], [7]. Cuckoo Search Algorithm (CS) [8]–[11]. Ant Lion Optimizer (ALO) [12], [13], Sine Cosine Algorithm (SCA) [14], [15], Salp Swarm Algorithm (SSA) [16], Whale Optimization Algorithm (WOA) [17], [18], Moth-Flame Optimization (MFO) [19], Poor and Rich Optimization (PRO) [20], Meerkats-inspired algorithm (MEA) [21], Kidney-inspired Algorithm [22], SailFish Optimizer (SFO) [23], Tree Growth Algorithm (TGA) [24], Squirrel Search Algorithm [25], Earthworm Optimization Algorithm [26]. So far, complex optimization problems have emerged endlessly,

and it is difficult to obtain optimal solutions. This is also an important reason why researchers are committed to practical optimization problems. There are many swarm intelligence algorithms that are widely used in combinatorial optimization [27], function optimization [28], multi-objective function optimization [29], three bar truss problems [30], cantilever beam design problems [31], gear system design problem [32]. However, there are still some limitations and unreliability in solving the practical optimization problems. Because of these limitations, many scholars have made further researches and improvements.

In the research of many scholars, the meta-heuristic algorithm is improved to avoid the problem of falling into local optimum. The Grey Wolf Optimizer (GWO) was proposed by Mirjalili [33], which is a new heuristic algorithm to solve the optimization problems. Shahrzad Saremi *et al.* proposed a new multi-objective grey wolf optimizer (MOGWO) to solve the challenging multi-objective optimization problems [34]. Hui Xu *et al.* proposed an improved GWO combined with cuckoo search aiming at the disadvantage that GWO is prone to fall into local optimum, especially when it is applied in high-dimensional data [35]. Teng Zhijun *et al.* proposed a hybrid grey wolf optimizer based on Tent mapping to increase global search capability [36]. Long and Wen proposed a new constrained optimization algorithm MAL-IGWO by combining the improved global optimization ability of the grey wolf optimization algorithm (IGWO) with the improved augmented Lagrangian multiplier method to deal with the constraint problems [37]. Li Shuxia *et al.* proposed an improved grey wolf optimizer (IGWO) based on evolution and elimination mechanism to achieve an appropriate compromise between exploration and development, further accelerate the convergence of exploration and development, and improve the optimization accuracy of GWO [38]. Kohli and Mehak introduced chaos theory into GWO to improve the global convergence rate [39]. MA Mushahhid proposed an improved typical enhanced grey wolf optimizer (EGWO), which improved the optimization ability of the algorithm and was successfully applied in analog circuits [40]. Jian Liu *et al.* proposed an improved double grey wolf optimizer [41]. E. Emary *et al.* proposed a variant of gray wolf optimization (GWO) that uses reinforcement learning principles combined with neural networks to enhance the performance [42]. Zawbaa *et al.* propose a combination of antlion optimization and grey wolf optimization in a new algorithm called ALO-GWO [43]. E. Emary and Zawbaa H M *et al.* proposed a novel binary version of the gray wolf optimization (GWO) and used it to select optimal feature subset for classification purposes [44]. Four bioinspired optimization algorithms: antlion optimization, binary version of antlion optimization, grey wolf optimization, and social spider optimization are used to select the optimal feature set for predicting the dissolution profile of PLGA by Zawbaa H M *et al.* [45]. Zawbaa H M *et al.* was found CI model shows that GWO algorithm is the most accurate method to predict porosity [46]. E. Emary *et al.* proposed an optimization algorithm based on two chaotic

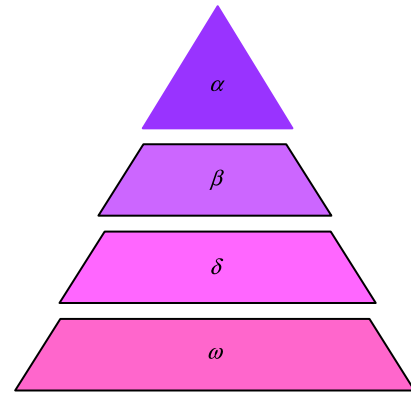
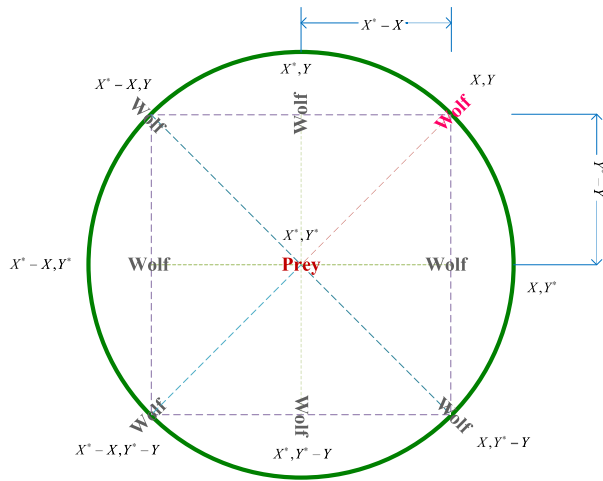


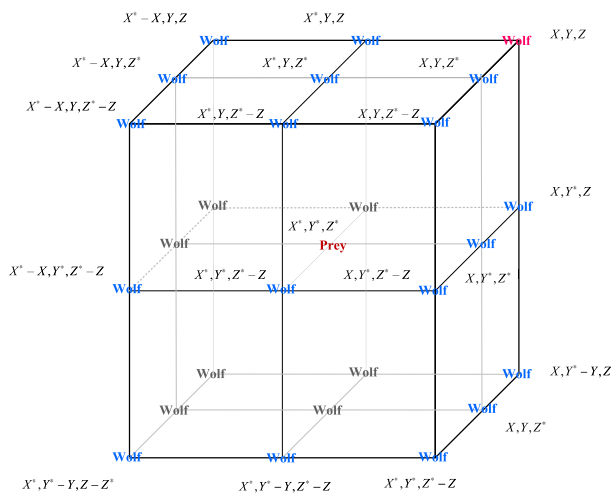
FIGURE 1. Mathematical model diagram.

functions that employed to analyze their performance and impact on grey wolf optimization, ant lion optimizer and moth-flame optimization [47]. E. Emary *et al.* proposed a classification accuracy-based fitness function by gray-wolf optimizer to find optimal feature subset [48]. Shubham Gupta *et al.* proposed a modified algorithm RW-GWO based on random walk [49]. Akash Saxena *et al.* presented an adaptive bridging mechanism based on β -chaotic sequence for the improvement of Grey Wolf Optimizer (GWO) [50].

Seeking mode and tracking mode were first proposed in cat swarm optimization (CSO) by Chu *et al.* [51]. Yang Shida *et al.* proposed a novel cat swarm algorithm based on the concepts of homotopy called a homotopy-inspired cat swarm algorithm (HCSA) [52]. Pei-Wei Tsai *et al.* investigated a parallel structure of cat swarm optimization and called it parallel cat swarm optimization (PCSO) [53]. Sharafi Y *et al.* presented a new algorithm binary discrete optimization method based on cat swarm optimization (BCSO) [54]. Ganapati Panda *et al.* developed a new learning rule based on population for the task definition model of IIR system identification using the recently introduced cat swarm optimization algorithm (CSO) [55]. An optimization method of parameter estimation of single diode and double diode model based on cat group optimization algorithm is proposed by Guo *et al.* [56]. An improved grey wolf optimizer based on tracking mode and seeking mode is proposed based on the three stages of encircling, tracking and attack of grey wolf aiming at the grey wolf optimizer has the disadvantage of easy convergence to local optimal. The algorithm is verified by simulation experiments in three parts. Firstly, the proposed tracking mode based grey wolf optimizer (TGWO), the seeking mode based grey wolf optimizer (SGWO), the tracking and seeking mode based grey wolf optimizer (TSGWO), Grey Wolf Optimizer (GWO), Particle Swarm Optimization (PSO), Salp Swarm Algorithm (SSA), Sine Cosine Algorithm (SCA), Ant Lion Optimizer (ALO), Whale Optimization Algorithm (WOA) and Moth-flame Optimization (MFO) are adopted to optimize 21 typical benchmark functions to show the effective of the proposed algorithms; Secondly, the improved algorithm proposed in



(a) 2D



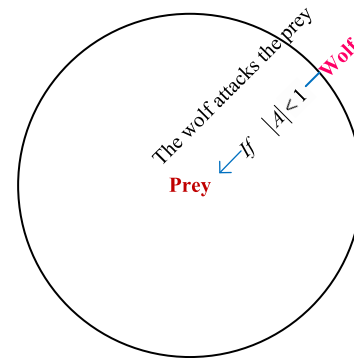
(b) 3D

FIGURE 2. 2D and 3D position vectors and their possible next locations.

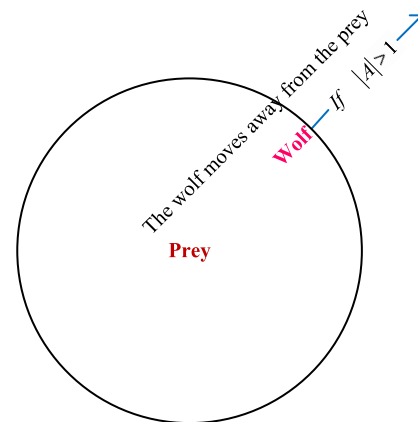
this paper is compared with Binary Grey Wolf Optimizer (BGWO), Hybrid PSO-GWO Optimization (PSO-GWO) and GWO Algorithm Integrated with Cuckoo Search (GWOCS); Finally, it is applied to the lightest design engineering problem of pressure vessels.

II. BASIC PRINCIPLE OF GWO

Grey wolf belongs to canine family. Most grey wolves prefer to live in groups. The grey wolves rely on a clear division of labor and cooperation to survive. Due to the clear division of labor, the gray wolf population is divided into four hierarchical systems. The leading grey wolf is called α wolf, its next level is called β wolf, the third level is called δ wolf, and the lowest level of the gray wolf is called ω wolf. The mathematical model established by the characteristics of the gray wolf swarm intermediate level is shown in Fig. 1. The grey wolf optimizer is a meta heuristic algorithm proposed



(a) $|A| < 1$



(b) $|A| > 1$

FIGURE 3. Attacking prey versus searching for prey.

in 2014. Grey wolf optimizer uses the characteristics of grey wolf social class to simulate its hunting mechanism. It is considered that three levels of wolves α , β and δ correspond to the three solutions with the best fitness. In each iteration, three wolves lead all wolves to a deeper exploration of the most likely searching space until the best position was found. The formula for the grey wolf surrounding the prey can be described as follows.

$$\vec{D} = \left| \vec{C} \cdot \vec{X}_p(t) - \vec{X}(t) \right| \quad (1)$$

$$\vec{X}(t+1) = \vec{X}_p(t) - \vec{A} \cdot \vec{D} \quad (2)$$

where t represents the algebraic number of the current iteration, $\vec{X}_p(t)$ characterizes the position vector of the prey, $\vec{X}(t)$ is the position vector reflecting the grey wolf, where both \vec{A} and \vec{C} refer to the coefficient vector, and they are calculated by:

$$\vec{A} = 2\vec{a} \cdot \vec{r}_1 - \vec{a} \quad (3)$$

$$\vec{C} = 2 \cdot \vec{r}_2 \quad (4)$$

$$a = 2 - 2 \left(\frac{t}{T_{\max}} \right) \quad (5)$$

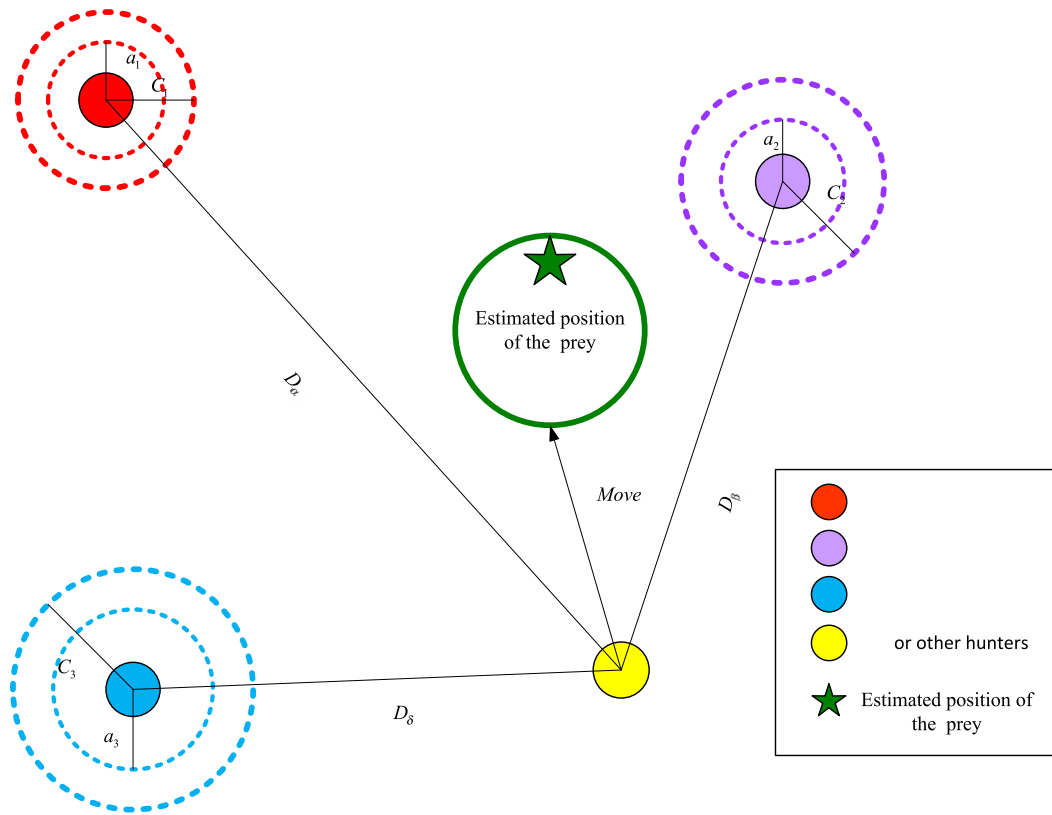


FIGURE 4. Location update of GWO.

where t represents the current number of iterations, T_{max} is the embodiment of the maximum number of iterations. It can be seen from the above formula that as the number of iterations increases, the convergence factor \vec{a} represents a value that gradually exhibits a linear decreasing trend from 2 to 0. \vec{r}_1 and \vec{r}_2 are random variables that are represented in the interval $[0, 1]$.

According to Eq. (1) and Eq. (2), the updating rule of the position of surrounding prey by grey wolves is presented. Fig. 2(a) shows the possible areas around the wolf when re-updating the position. It can be seen from Fig. 2(a) that the grey wolf in position (X, Y) can re-position the position according to the location (X^*, Y^*) of the prey. At each iteration, the position vector of the grey wolf is updated by constantly adjusting the values of \vec{A} and \vec{C} , so that the grey wolf can go anywhere near the prey. The 3-dimensional position update of the grey wolf is shown in Fig. 2(b). The presence of the random variables \vec{r}_1 and \vec{r}_2 allows the grey wolf position to be updated to any position according to Eq. (1) and (2).

It is worth noting that the convergence factor \vec{a} is a variable that decreases linearly with the number of iterations from 2 to 0. According to Eq. (3), \vec{A} is a random variable between $[-2a, 2a]$. In this case, it is necessary to divide into two cases according to the range of \vec{A} . It can be seen from Fig. 3(a) that When \vec{A} is between $[-1, 1]$, the next generation can

update the position arbitrarily between the current location and the location of the prey. When $|A| < 1$, the grey wolf attacks the prey at this time. This situation is more indicative of the development capability of gray wolf, but these random vectors proposed so far may make it easy to fall into local optimal. It can be seen from Fig. 3(b) that when the random variable \vec{A} is between $[-\infty, -1]$ or $[1, \infty]$, the grey wolf will not attack the prey. That is to say when $|A| > 1$, the grey wolf will force the current agent to stay away from the prey and search for more suitable prey. Random variable \vec{C} can also improve the exploration ability of the algorithm. It can be seen from Eq. (4) that \vec{C} is a random variable, and there is no random linear reduction. The randomness is maintained from the initial iteration to the final iteration, which improves the global optimization ability of the final iteration.

The grey wolf population is divided into four grades α, β, δ and ω . The first three grades α, β and δ are in corresponding to the three solutions with the best fitness. Then the wolf positions with these three grades are updated by adopting the following formula.

$$\vec{D}_\alpha = \left| \vec{C}_1 \cdot \vec{X}_\alpha - \vec{X} \right| \tag{6}$$

$$\vec{D}_\beta = \left| \vec{C}_2 \cdot \vec{X}_\beta - \vec{X} \right| \tag{7}$$

$$\vec{D}_\delta = \left| \vec{C}_3 \cdot \vec{X}_\delta - \vec{X} \right| \tag{8}$$

where \vec{X}_α is the position vector of α wolf, \vec{X}_β is the position vector of β wolf, and \vec{X}_δ represents the position vector of δ wolf.

Under normal circumstances, it is assumed that the first three levels of grey wolves know the general position of the prey on the way of hunting. After obtaining the above position vector, the wolves will perform the final update according to the obtained position by adopting the following formula.

$$X_1 = |X_\alpha - A_1 \cdot D_\alpha| \quad (9)$$

$$X_2 = |X_\beta - A_2 \cdot D_\beta| \quad (10)$$

$$X_3 = |X_\delta - A_3 \cdot D_\delta| \quad (11)$$

$$X_{(t+1)} = \frac{X_1 + X_2 + X_3}{3} \quad (12)$$

The position update principle of the algorithm is shown in Fig. 4. During each iteration update, the position of the grey wolf is estimated by the best three levels of positions. $X_{(t+1)}$ is the updated position of the next generation of wolves, and each candidate solution will update the distance between them and the prey [57]. In summary, the grey wolf optimizer begins to randomly initialize the population, and then updates the position of the candidate solution each according to the three wolves with the best fitness, namely, α wolf, β wolf, and δ wolf. The range of the random variable $|A| < 1$ determines that the wolf is approaching the prey, $|A| > 1$ indicates that the wolf is forced to stay away from the prey to find a more suitable prey, and converges to the optimal solution in the last iteration.

III. IMPROVED GREY WOLF OPTIMIZER BASED ON TRACKING MODE AND SEEKING MODE

A. TRACKING MODE AND SEEKING MODE

According to the high alertness of cats in idle state and the characteristics of tracking dynamic targets, a cat swarm algorithm based on seeking mode and tracking mode was proposed in 2006. In this paper, tracking mode and seeking mode are integrated into grey wolf optimizer to improve the randomness of its search. The improved algorithm realizes the balance of exploitation and exploration, and is not easy to fall into the local optimal solution.

The tracking mode is a kind of simulation of the state of a wolf when it is tracking a dynamic target. It mainly applies the update of velocity and position of each dimension to change the position with random disturbance. The tracking mode is implemented by adopting the following steps.

Step 1: Calculate the speed of the i_{th} Wolf in each dimension according to the following formula:

$$v_{i,d}(t+1) = v_{i,d}(t) + r \times C \times (X_{best,d}(t) - x_{i,d}(t)) \quad (13)$$

where $X_{best,d}(t)$ is the best position for the wolf currently available, $d = 1, 2, \dots, M$, $x_{i,d}(t)$ indicates the location of the i_{th} wolf, r and C are random variables located in the scope $[0, 1]$.

Step 2: Update the location by the following formula:

$$x_{i,d}(t+1) = x_{i,d}(t) + v_{i,d}(t+1) \quad (14)$$

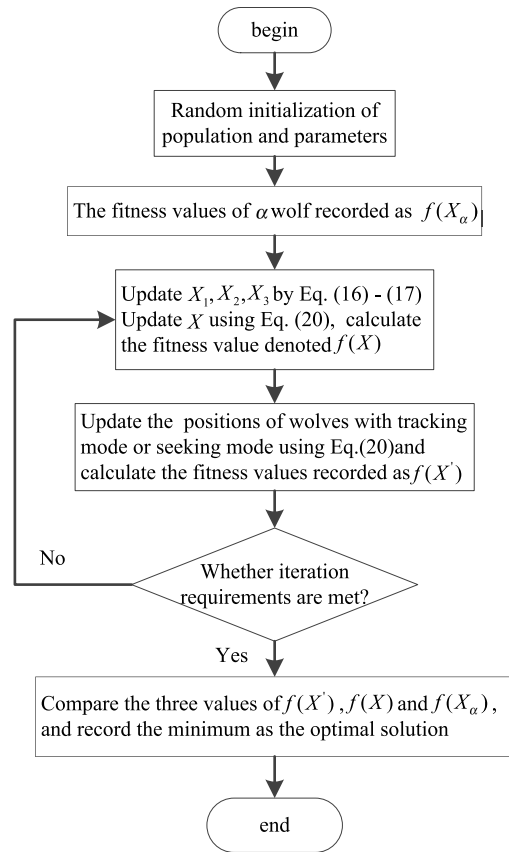


FIGURE 5. Flowchart of GWO based on tracking mode and seeking mode.

where $x_{i,d}(t+1)$ represents the updated position of the wolf at the next iteration.

The seeking mode is recorded by the four elements (memory pool SMP , the change field SRD , the change number CDC , and the judgment of its own position SPC). The memory pool (SMP) describes the size of each wolf's search memory, which is mainly used to find the location with the best fitness. The variation domain (SRD) generally has a value of 0.2, which plays a decisive role in the changing range of each dimension. The number of changes (CDC) is the number of dimensions of the wolf variation in each generation. SPC is defined as a Boolean value that determines whether the position passed by the current iteration can be used as a candidate solution. However, No matter the value of SPC is true or false; the value of SMP will not be influenced. The specific steps of the seeking mode can be described as follows.

Step 1: Put the complete positions in the current iteration into the memory pool (SMP) with N copies, where N is the size of the memory pool. If SPC is true, then let $N = SMP - 1$; if SPC is false, then let $N = SMP$ and use the position in the current iteration as a candidate solution.

Step 2: Change the dimension of each wolf in the memory pool (SMP). So a perturbation is produced in the dimension,

TABLE 1. Parameter settings for each algorithm.

Algorithm	Main parameters Settings
PSO	Particle number $n = 30$; Learning factor $c_1 = 2$, $c_2 = 2$; Inertia weight $w_{Max} = 0.9$, $w_{Min} = 0.9$
SSA	Population size $n = 30$
SCA	Population size $n = 30$; $a = 2$
ALO	Population size $n = 30$
WOA	Population size $n = 30$; $b = 1$; a variable decreases linearly from 2 to 0 (Default) a2 linearly decreases from -1 to -2 (Default)
MFO	population size $n = 30$
GWO	Wolves number $n = 30$; a variable decreases linearly from 2 to 0 (Default)
TGWO	Wolves number $n = 30$
SGWO	Wolves number $n = 30$; $SRD = 0.25$; $SMP = 5$; $CDC = 0.65$
TSGWO	Wolves number $n = 30$; $SRD = 0.25$; $SMP = 5$; $CDC = 0.65$

that is to say:

$$dim = (1 \pm rand \cdot SRD) \cdot dim_{sel} \tag{15}$$

where dim_{sel} is the number of dimensions selected to be changed, SRD represents the control range of the dimensional change of each individual, $SRD = 0.25$ in this paper, $rand$ is a uniformly distributed random number between $[0, 1]$.

Step 3: Calculate the fitness values of all the found candidate solutions in the memory pool.

Step 4: Among the optimal candidate values of the calculated fitness values, the position of the optimal candidate is taken as the position of the current individual.

According to the grey wolf optimizer, Each iteration will update the position of α wolf, β wolf and δ wolf. As the iteration continues and the problem has the higher dimension, grey wolf optimizer may fall into local optimum. In this paper, tracking mode and seeking mode are used to interfere the grey wolf optimizer algorithm randomly, and three improved strategies are proposed. The first strategy is the grey wolf optimizer based on tracking mode (TGWO). Integrate the tracking mode into the grey wolf optimizer using Eq. (13) and (14) to make the wolf's position X_α , X_β , and X_δ interfered and updated to increase their global search ability. The second strategy is the grey wolf optimizer based on seeking mode (SGWO). This specific method is to separately add the seeking mode to the grey wolf optimizer. The best three solutions plus the disturbance. After using the seeking mode to determine its position, Eq. (15) is adopted to randomly change the candidate solution, and select the candidate with the highest fitness value to replace the current wolf position. The third strategy is the grey wolf optimizer based on tracking

and the seeking mode (TSGWO). The tracking mode is used to update the position X_α of the α wolf, the seeking mode is used to update the positions X_β and X_δ of the β wolf and the δ wolf. The improved grey wolf optimizer improves the convergence accuracy and avoids the situation of falling into local optimum.

B. IMPROVED ALGORITHM FLOW

The algorithm procedure of the grey wolf optimizer based on the tracking mode and the seeking mode is described as follows.

Step 1: Initialize the algorithm control parameters: population size ($SearchAgents_no$), the maximum iteration number ($Max_iteration$), memory pool (SMP), number of changes (CDC), each individual's change domain (SRD), random initialization speed, random positions of α wolf, β wolf and δ wolf ($Alpha_pos$, $Beta_pos$, $Delta_pos$).

Step 2: update the positions of α wolf, β wolf and δ wolf using Eq. (9) - (11). Calculate the fitness value of all wolves, Set the X_α as the best search agent, and calculate the fitness value $f(X_\alpha)$.

Step 3: TGWO algorithm uses Eq. (16) and (17) to update the positions of α wolf, β wolf and δ wolf. AGWO algorithm updates the α wolf using the seeking pattern and updates β wolf and δ wolf with the tracking mode by using Eq. (16) and Eq. (18); SGWO algorithm uses the seeking mode to update the positions of α wolf, β wolf and δ wolf, Copy the individuals in the current seeking mode to generate a series of individuals to fill the search memory pool: X_1 , X_2 and X_3 are liberated into the memory pool as candidates, setting $SMP = 5$, At this time, the candidate solution is copied N copies by

TABLE 2. Benchmark functions.

Function	Dim	Range	f _{min}
$F_1 \ x = \sum_{j=1}^n x_j^2$	30,100	[-100,100]	0
$F_2 \ x = \sum_{i=1}^n x_i + \prod_{i=1}^n x_i $	30,100	[-10,10]	0
$F_3 \ x = \sum_{i=1}^n \sum_{j=1}^i x_j^2$	30,100	[-100,100]	0
$F_4 \ x = \max \{x_i\}, 1 \leq i \leq n$	30,100	[-100,100]	0
$F_5 \ x = \sum_{i=1}^{n-1} [100 \ x_{i+1} - x_i^2 + x_i^{-1}^2]$	30,100	[-30,30]	0
$F_6 \ x = \sum_{i=1}^n x_i + 0.5^2$	30,100	[-100,100]	0
$F_7 \ x = \sum_{i=1}^n ix_i^4 + random \ 0,1$	30,100	[-1.28,1.28]	0
$F_8 \ x = \sum_{i=1}^n -x_i^2 \sin \sqrt{ x_i }$	30,100	[-500,500]	-418.9829×Dim
$F_9 \ x = \sum_{i=1}^n [x_i^2 - 10 \cos \ 2\pi x_i + 10]$	30,100	[-5.12,5.12]	0
$F_{10} \ x = -20 \exp \left(-0.2 \sqrt{\frac{1}{n} \sum_{i=1}^n x_i^2} \right) - \exp \left(\frac{1}{n} \sum_{i=1}^n \cos \ 2\pi x_i \right) + 20 + e$	30,100	[-32,32]	0
$F_{11} \ x = \frac{1}{4000} \sum_{i=1}^n x_i^2 - \prod_{i=1}^n \cos \left(\frac{x_i}{\sqrt{i}} \right) + 1$	30,100	[-600,600]	0
$F_{12} \ x = \frac{\pi}{n} 10 \sin \ \pi y_i + \sum_{i=1}^{n-1} y_i^{-1} [1 + 10 \sin^2 \ \pi y_{i+1}] + \sum_{i=1}^n u \ x_i, 10, 100, 4$ $y_i = 1 + \frac{x_i + 1}{4}, u \ x_i, a, k, m = \begin{cases} k \ x_i - a^{-m} & x_i > a \\ 0 & -a < x_i < a \\ k \ -x_i - a^{-m} & x_i < -a \end{cases}$	30,100	[-50,50]	0
$F_{13} \ x = 0.1 \{ \sin^2 \ 3\pi x_1 + \sum_{i=1}^n x_i^{-1} [1 + \sin^2 \ 3\pi x_i + 1] + x_n^{-1} [1 + \sin^2 \ 2\pi x_n] \} + \sum_{i=1}^n u \ x_i, 5, 100, 4$	30,100	[-50,50]	0
$F_{14} \ x = \left(\frac{1}{500} + \sum_{j=1}^{25} \frac{1}{j + \sum_{i=1}^2 x_i - a_{ij}^6} \right)^{-1}$	2	[-65,65]	1
$F_{15} \ x = -\sum_{i=1}^5 [X - a_i \ X - a_i^r + c_i]^{-1}$	4	[0,10]	-10.1532
$F_{16} \ x = -\sum_{i=1}^7 [X - a_i \ X - a_i^r + c_i]^{-1}$	4	[0,10]	-10.4028
$F_{17} \ x = -\sum_{i=1}^{10} [X - a_i \ X - a_i^r + c_i]^{-1}$	4	[0,10]	-10.5363
$F_{18} \ x = x_1^2 + 10^6 \sum_{i=2}^D x_i^2$	30,100	[-10,10]	0
$F_{19} \ x = \sum_{i=1}^D x_i ^{1.1}$	30,100	[-100,100]	0
$F_{20} \ x = \sum_{i=1}^D x_i^2 + \sum_{i=1}^D 0.5x_i^2 + \sum_{i=1}^D 0.5x_i^4$	30,100	[-5,10]	0
$F_{21} \ x = \sin^2 \ \pi w_1 + \sum_{i=1}^D w_i^{-1} [1 + 10 \sin^2 \ \pi w_i + 1] + w_D^{-1} [1 + \sin^2 \ 2\pi w_D]$ <i>Where</i> $w_i = 1 + \frac{x_i - 1}{4}, \forall i = 1, \dots, D$	30,100	[-10,10]	0

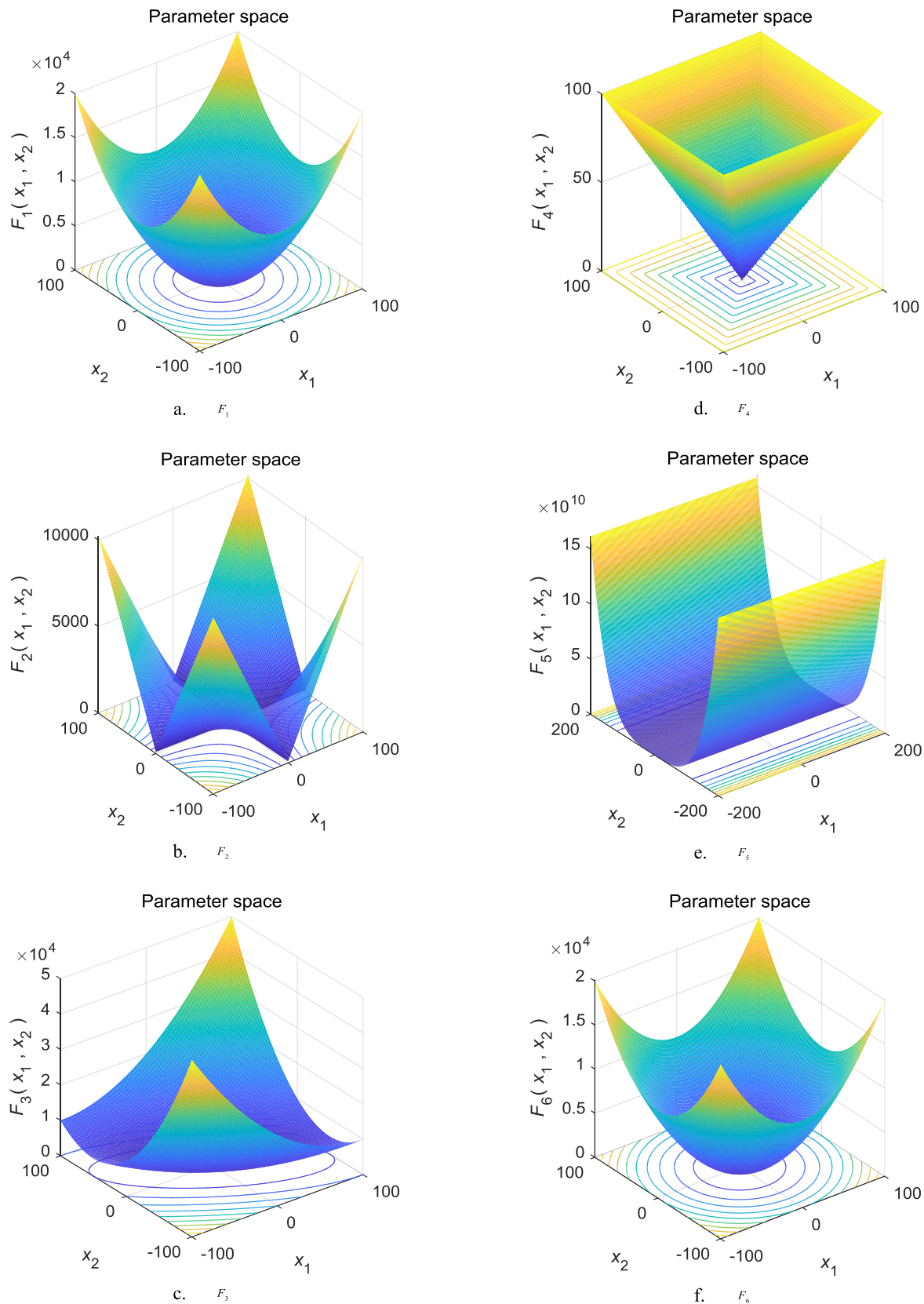


FIGURE 6. Three-dimensional images of the test functions.

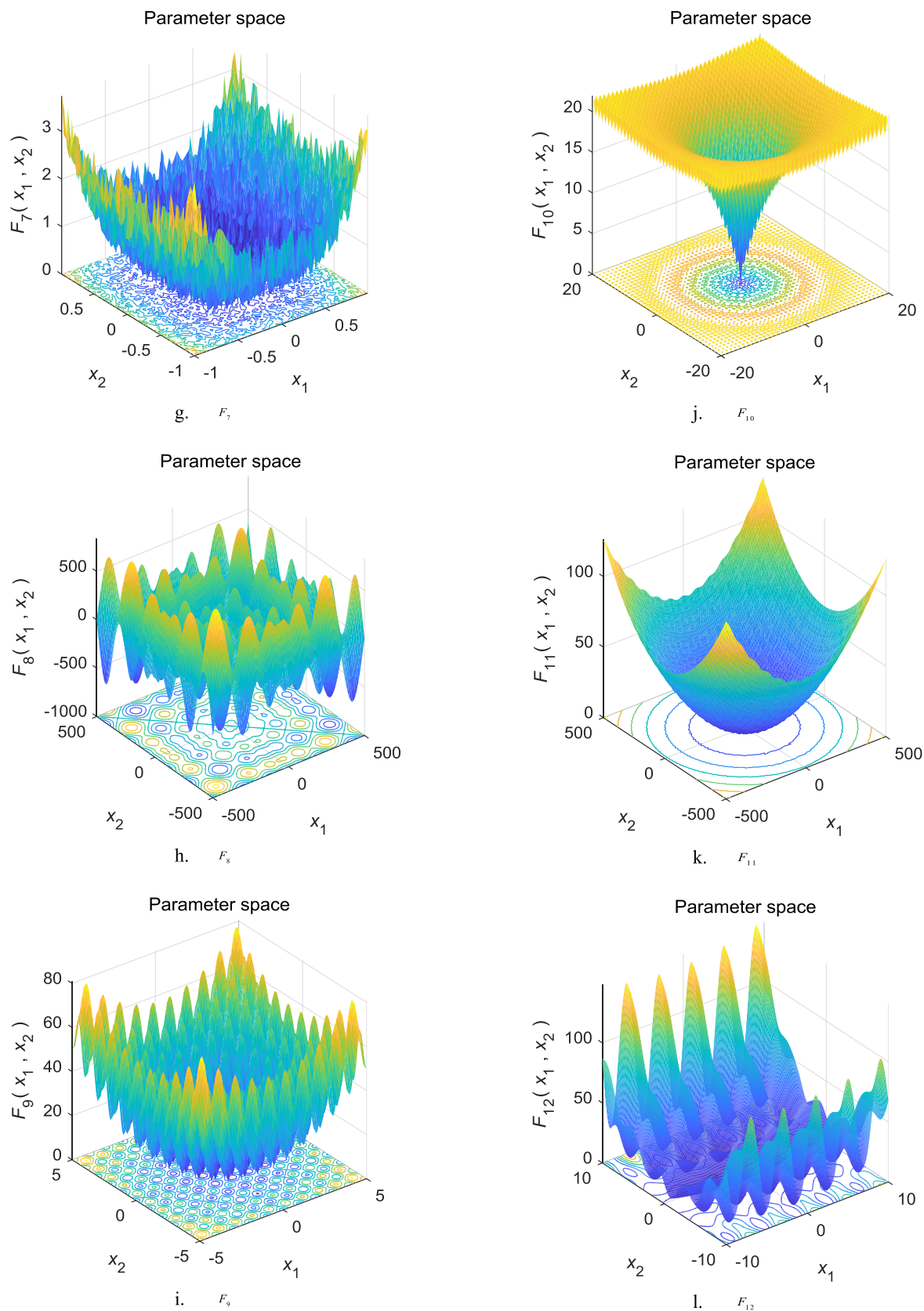


FIGURE 6. (continued.) Three-dimensional images of the test functions.

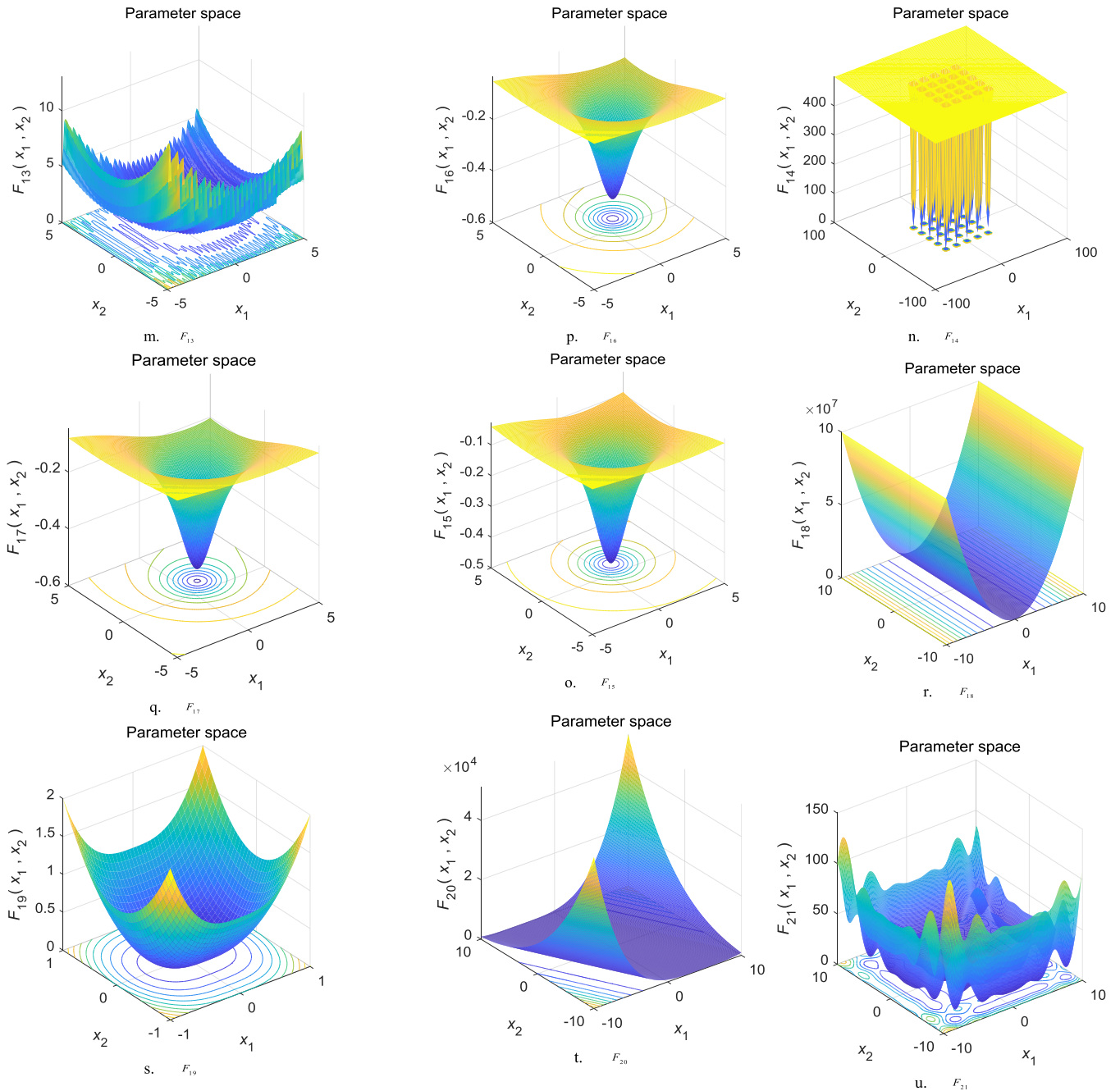


FIGURE 6. (continued.) Three-dimensional images of the test functions.

Eq. (18), $N = SMP - 1$; the fitness values of all candidate points in the memory pool are calculated separately; Execute mutation operator. The change range of each dimension is determined by the change field SRD , setting $SRD = 0.25$; For each individual in the memory pool, set $CDC = 0.65$ according to the size of the CDC , and select the dimension to be randomly changed by Eq. (19); Add a disturbance to the original position according to Eq. (15) and reach the new position to replace the original position; Recalculate the fitness values of all candidate solutions in the memory

pool after changing dimensions; The candidate point with the highest fitness value is selected from the memory pool to replace the current wolf position.

$$v_i(t + 1) = v_i(t) + r_i \times C_i \times (X_i(t) - x_i(t)) \quad (16)$$

$$X_i(t + 1) = X_i(t) + v_i(t + 1) \quad (17)$$

$$Wolf_C = repmat(X1(i, :), SMP - 1, 1) \quad (18)$$

$$Dims_Changed = round(CDC * size(Wolf_C, 2)) \quad (19)$$

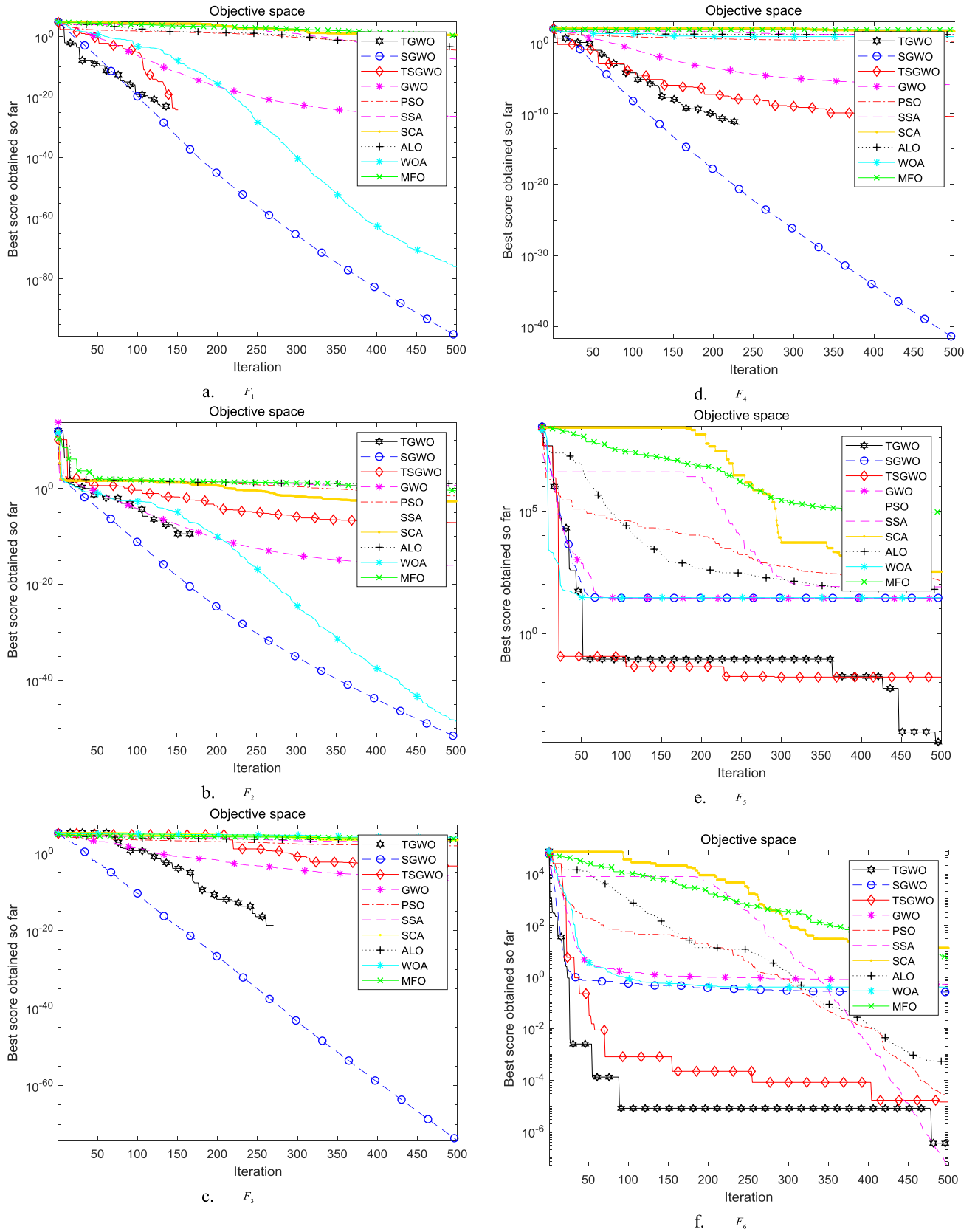


FIGURE 7. Simulation results of function F_1 - F_{13} and F_{18} - F_{21} with 30 dimension.

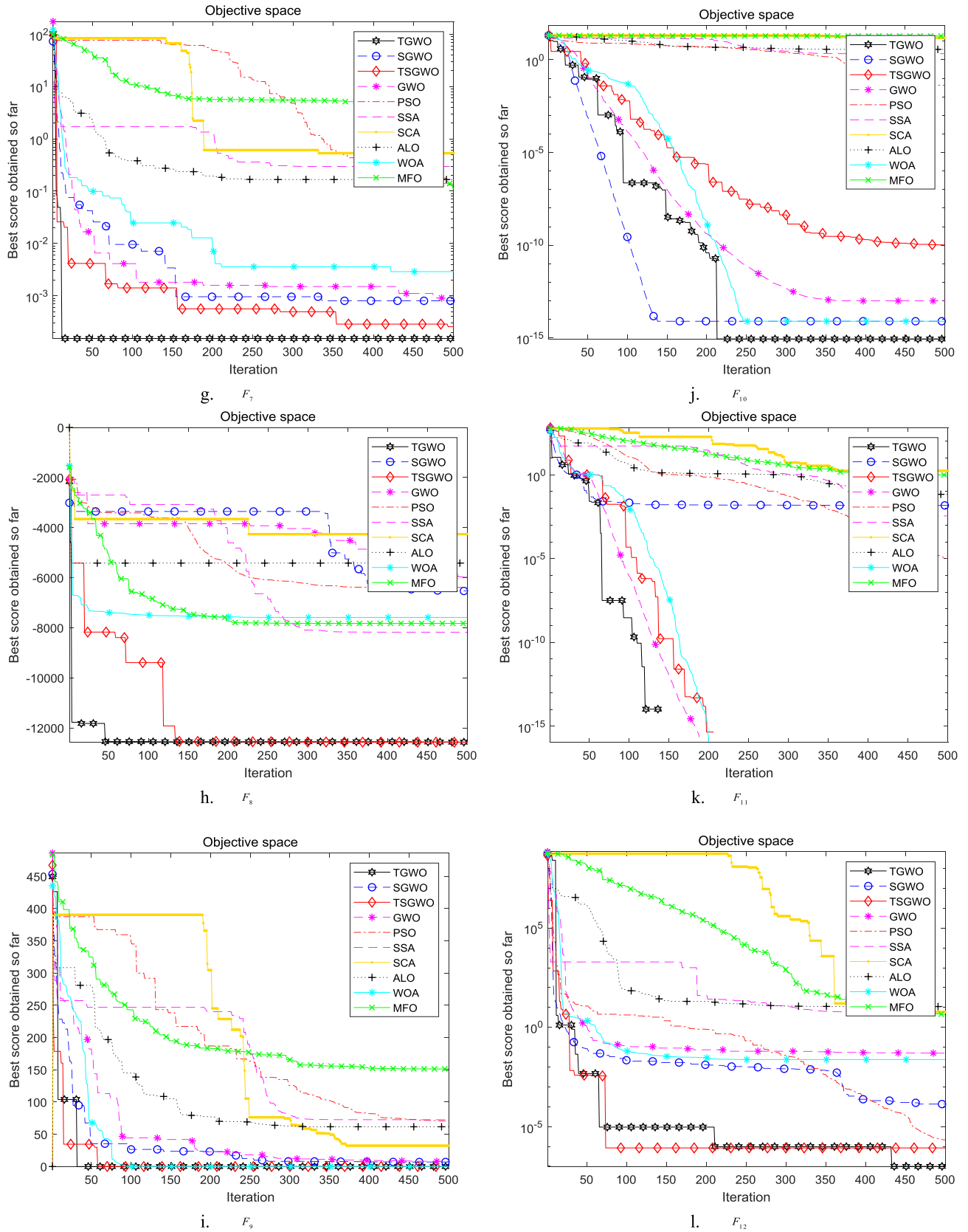


FIGURE 7. (continued.) Simulation results of function F_1 - F_{13} and F_{18} - F_{21} with 30 dimension.

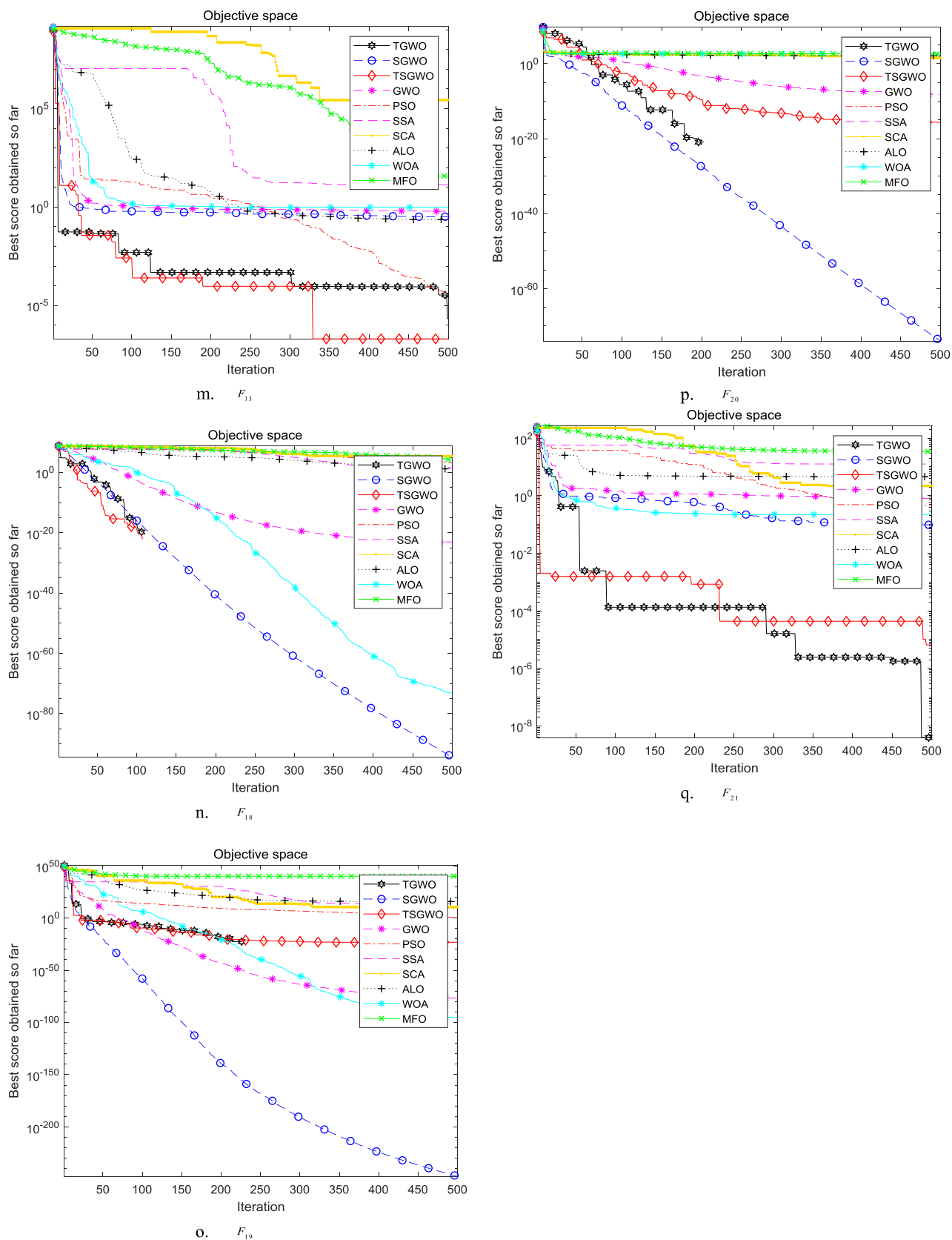


FIGURE 7. (continued.) Simulation results of function F_1 - F_{13} and F_{18} - F_{21} with 30 dimension.

TABLE 3. Running results of functions under 30 dimension.

Function	TGWO	TSGWO	SGWO	GWO	SSA	SCA	PSO	ALO	WOA	MFO	
F_1	Best	0	0	2.79E-100	5.82E-29	2.90E-08	0.195332	6.54E-06	0.0001169	4.214E-85	0.9075692
	Ave	0	1.00E-18	6.60E-99	1.617E-27	1.83E-07	8.96E+00	0.0001746	0.0003982	2.026E-80	13.227273
	Std	0	3.160E-18	1.171E-98	1.283E-27	1.732E-07	9.968776	0.0001937	0.0001835	3.692E-80	34.808477
F_2	Best	0	0	6.37E-53	3.21E-17	0.331969	0.0005744	0.003112	0.9350286	5.583E-59	0.1153384
	Ave	0	4.092E-11	1.405E-52	7.721E-17	2.20282	0.0144625	0.039973	8.9422360	1.010E-51	14.205513
	Std	0	5.215E-11	5.872E-53	3.527E-17	2.362473	0.0329405	0.040444	6.3196253	2.953E-51	11.893920
F_3	Best	0	0	5.34E-79	9.66E-10	654.5558	2883.83	32.34513	956.78993	27204.033	4377.5296
	Ave	0	9.13E-09	2.88E-75	8.63E-07	1578.76	9.15E+03	79.96155	2741.9721	36445.254	15790.589
	Std	0	2.564E-08	7.51E-75	1.52E-06	662.842	5806.795	45.02691	965.97079	6384.1601	6863.0973
F_4	Best	0	0	1.30E-43	1.84E-07	8.755386	15.25491	0.6785	10.554740	2.4053186	53.187134
	Ave	0	7.573E-11	6.204E-43	8.045E-07	13.74441	29.38021	1.068826	17.782633	40.535836	63.724796
	Std	0	1.203E-10	6.830E-43	6.057E-07	4.111726	9.476234	0.255725	4.2971303	26.586182	6.5448995
F_5	Best	2.37E-07	4.49E-06	25.8829	26.17555	24.87873	107.4604	22.31532	29.363885	27.278986	248.41469
	Ave	7.92E-05	1.62E-03	2.74E+01	2.73E+01	9.93E+01	1.88E+04	6.74E+01	122.54220	28.051537	1838.5286
	Std	8.479E-05	0.002978	0.864968	0.619309	124.7004	38383.24	35.68103	119.98182	0.5417770	1460.2483
F_6	Best	3.117E-09	7.323E-09	0.002881	0.500383	3.263E-08	7.176993	1.56E-05	0.0002658	0.1983505	0.1853476
	Ave	1.599E-06	5.149E-06	0.053341	0.817699	1.108E-07	38.5008	0.000269	0.0008498	0.3813812	2002.8560
	Std	2.065E-06	1.148E-05	0.10519	0.246303	8.103E-08	94.14311	0.000402	0.0004004	0.1357736	5999.5029
F_7	Best	5.690E-07	4.086E-05	0.000475	0.001117	0.059648	0.006006	0.103299	0.1532049	0.0007624	0.0881736
	Ave	8.692E-05	0.0001210	0.001414	0.001959	0.136926	0.060517	0.181315	0.2351979	0.0041435	0.5147165
	Std	6.968E-05	7.908E-05	0.000815	0.000819	0.068898	0.062791	0.054078	0.0996353	0.0036105	0.8451515
F_8	Best	-12569.5	-12569.5	-6735.106	-6768.172	-8784.57	-3882.597	-7638.091	-5537.590	-12566.06	-10612.57
	Ave	-11503.5	-11148.1	-6001.571	-6018.928	-7428.52	-3627.486	-5091.296	-5441.481	-10397.33	-9073.564
	Std	1716.379	1834.979	552.23408	647.88616	1080.204	204.48845	1578.2801	47.615282	1809.0471	803.08254
F_9	Best	0	0	0.00E+00	5.68E-14	32.8336	3.16E+00	38.96274	53.727837	0	89.635451
	Ave	0	1.022E-07	1.50E+00	3.35E+00	52.63324	5.07E+01	5.77E+01	78.404866	5.684E-15	141.58554
	Std	0	3.234E-07	1.956328	4.822554	13.20332	41.38622	12.1188	26.289854	1.705E-14	29.697473
F_{10}	Best	8.88E-16	8.881E-16	7.99E-15	8.62E-14	1.646224	5.33E-02	0.004539	2.1216717	8.881E-16	14.825173
	Ave	8.881E-16	2.467E-11	7.99E-15	1.12E-13	2.609253	1.11E+01	4.33E-01	5.8435695	5.506E-15	19.112821
	Std	6.573E-32	3.587E-11	1.05E-30	1.76E-14	0.71748	9.765001	0.733236	3.6294184	2.274E-15	1.5395566
F_{11}	Best	0	0	0.00E+00	0.00E+00	0.002536	7.98E-01	1.25E-06	0.0148542	0	0.7097404
	Ave	0	0	1.99E-03	3.81E-03	0.022256	1.02E+00	5.94E-03	0.0500318	0	9.9293107
	Std	0	0	0.006293	0.008481	0.019856	0.195334	0.007173	0.0213329	0	27.033086
F_{12}	Best	3.355E-10	1.279E-09	9.17E-05	2.39E-02	1.974136	0.657465	1.55E-07	6.5800303	0.0069047	1.7587933
	Ave	6.281E-08	2.118E-07	3.39E-03	4.27E-02	5.568869	1.30E+01	1.04E-02	15.667029	0.0352640	61.055105
	Std	8.530E-08	4.813E-07	0.004651	0.023455	3.737769	16.90091	0.032783	8.6447598	0.0296122	161.65207
F_{13}	Best	1.007E-08	2.353E-09	5.35E-03	4.05E-01	0.078634	5.034696	3.33E-05	1.2976399	0.2485014	4.0542760
	Ave	3.200E-06	2.360E-06	3.01E-01	6.34E-01	13.225	3.51E+01	4.70E-03	31.658018	0.6593188	22.715000
	Std	6.437E-06	2.437E-06	0.172903	0.17847	17.28735	44.81446	0.006002	18.746344	0.2655951	18.883737
F_{18}	Best	0	0	9.53E-97	1.671E-25	0.0228640	2656.0544	11.676115	9.5131894	1.373E-77	5619.4238
	Ave	0	3.922E-16	4.45E-95	1.352E-23	9.7245396	82075.585	64.877262	22.582116	1.926E-73	4.00E+07
	Std	0	8.764E-16	5.11E-95	1.723E-23	12.321145	86580.211	46.176499	10.482903	5.382E-73	48982034.
F_{19}	Best	0	0	1.30E-249	2.220E-89	7.55E+08	510.48341	0.0003005	4.91E+11	3.69E-112	1.00E+28
	Ave	0	1.793E-20	3.44E-242	2.242E-78	3.15E+18	2.71E+14	0.1459996	3.20E+20	3.294E-90	3.04E+41
	Std	0	5.204E-20	0	5.879E-78	7.74E+18	8.15E+14	0.2481978	8.15E+20	9.883E-90	4.57E+41
F_{20}	Best	0	0	2.84E-76	6.936E-09	15.172861	6.1371052	53.555629	111.52966	332.19479	75.268451
	Ave	0	4.759E-17	6.86E-74	2.507E-07	43.390398	34.184845	73.272650	175.80574	500.04063	345.30546
	Std	0	9.517E-17	1.60E-73	5.086E-07	28.924671	21.178262	15.970529	47.438025	105.47726	137.10210
F_{21}	Best	3.95E-09	2.34E-09	7.06E-03	7.25E-01	3.08E+00	2.19E+00	2.19E-03	4.57E+00	2.22E-01	5.77E+00
	Ave	3.07E-06	7.49E-06	2.06E-01	1.06E+00	8.14E+00	6.10E+00	5.82E-01	1.11E+01	4.97E-01	2.61E+01
	Std	3.856E-06	1.513E-05	0.1057708	0.2888095	2.9963920	3.2495081	0.6219507	4.0583341	0.1537388	10.040314

TABLE 4. Running results of functions under 100 dimension.

Function	TGWO	TSGWO	SGWO	GWO	SSA	SCA	PSO	ALO	WOA	MFO	
F_1	Best	0	0	3.61E-84	3.15E-13	964.8583	5704.004	13.820168	2420.1172	1.452E-78	37415.634
	Ave	0	6.379E-19	1.71E-83	1.42E-12	1538.093	1.39E+04	21.191807	4695.8036	1.211E-71	62663.591
	Std	0	1.509E-18	8.903E-84	8.495E-13	461.7767	5796.002	4.6512093	1496.3256	2.896E-71	18826.414
F_2	Best	0	0	7.56E-44	2.31E-08	39.92937	1.63E+00	23.665525	63.383628	1.820E-52	189.48425
	Ave	0	3.547E-10	1.83E-43	4.33E-08	46.13192	6.146539	31.594800	1.79E+11	1.203E-50	246.48627
	Std	0	4.940E-10	6.92E-44	1.47E-08	4.191445	3.310207	5.5472839	5.37E+11	2.000E-50	54.195437
F_3	Best	0	0	1.10E-69	5.02E+01	16499.36	208749.8	7930.8531	59213.238	693861.26	158097.27
	Ave	0	6.620789	1.51E-67	573.2178	48375.58	263542	18226.556	94690.572	1025333.6	245488.28
	Std	0	20.79827	1.92E-67	522.0657	16688.81	68616.25	6545.2962	22103.828	160818.64	46743.454
F_4	Best	0	0	3.72E-38	0.079339	22.24432	86.09819	10.540775	26.705430	7.5631922	92.129072
	Ave	0	6.191E-10	7.45E-38	0.884038	27.34708	89.73383	12.339939	34.814183	73.350592	95.448008
	Std	0	1.489E-09	4.45E-38	0.63817	3.14129	2.373459	1.2215607	6.3318671	26.591124	1.5698057
F_5	Best	5.28E-08	7.68E-05	9.70E+01	9.69E+01	92212.47	27461817	13583.896	302430.82	98.076028	51057038
	Ave	2.94E+01	19.60225	9.81E+01	97.82901	1.76E+05	1.2E+08	17540.139	836144.95	98.238416	1.72E+08
	Std	47.33739	41.31913	0.489007	0.710188	77177.2	78347258	2990.5381	467773.61	0.0963157	7.08E+07
F_6	Best	3.489E-08	2.093E-09	3.49E-03	6.09E-05	5.89E-08	9.93E+00	13.990453	1376.1928	1.1054568	57584.751
	Ave	1.979E-06	3.285E-06	0.416697	8.601334	949.9288	5245.439	18.107006	3968.5463	3.7735170	69747.960
	Std	3.077E-06	2.829E-06	0.360974	4.129012	632.1247	3761.676	3.9466099	1747.6287	1.4503542	10333.888
F_7	Best	1.239E-05	1.257E-05	2.71E-03	3.40E-03	2.046461	53.10694	909.51642	3.1638287	9.158E-05	124.19764
	Ave	7.255E-05	9.029E-05	0.005387	0.008377	2.854522	138.0998	1532.9279	5.5269820	0.0029899	229.15439
	Std	7.463E-05	8.484E-05	0.002386	0.004266	0.917	78.46461	303.54847	2.0478468	0.0034302	90.021884
F_8	Best	-41898.3	-41898.3	-20042.99	-1.72E+04	-25038.3	-8190.019	-19228.12	-18058.91	-41885.26	-28149.37
	Ave	-40713.4	-35976.3	-17378.96	-15245.46	-22211.6	-6689.748	-10590.02	-18058.91	-38153.02	-22689.77
	Std	3745.167	6242.233	1517.1949	3274.6650	1717.341	612.26232	4496.3193	0	5006.9570	2209.7822
F_9	Best	0	0	0.00E+00	1.14E-13	34.82354	9.19E+00	459.24644	338.22941	0	706.01226
	Ave	0	0.015555	1.704361	9.080816	156.386	190.2263	555.89989	382.08080	0	870.60070
	Std	0	0.049188	2.370799	8.850257	89.52753	201.4854	69.102650	27.356883	0	78.100450
F_{10}	Best	8.881E-16	8.881E-16	1.51E-14	5.06E-08	8.230765	2.06E+01	3.0896730	12.991437	8.881E-16	19.356818
	Ave	3.039E-13	7.198E-10	1.51E-14	1.14E-07	10.30827	20.61045	3.6912913	14.163230	5.151E-15	19.829773
	Std	7.689E-13	1.550E-09	0	3.6E-08	0.909994	0.040982	0.4144887	0.7287450	2.658E-15	0.1819103
F_{11}	Best	0	0	0	1.27E-13	6.864723	3.05E+01	0.2625824	16.345451	0	349.95748
	Ave	0	0	0	0.00489	14.51732	102.2161	0.3892669	55.266971	0	554.60813
	Std	0	0	0	0.010459	5.56931	58.154	0.0875299	19.086261	0	162.55324
F_{12}	Best	1.513E-09	4.498E-10	1.82E-04	1.33E-01	17.54964	6.04E+08	2.6028788	60.699030	0.0350445	89021494.
	Ave	4.263E-08	6.338E-08	0.009242	0.275197	34.20209	3.04E+08	4.7539232	102.63958	0.0464105	3.05E+08
	Std	5.423E-08	1.219E-07	0.006104	0.064826	16.1037	1.84E+08	1.8028623	64.657189	0.0097312	1.63E+08
F_{13}	Best	1.944E-11	6.468E-07	3.84E+00	5.26E+00	185.2117	9.91E+07	46.904865	8991.9040	1.8107712	3.18E+08
	Ave	4.482E-06	7.181E-06	4.172949	6.586583	15005.95	4.87E+08	68.382338	271844.37	2.8794325	8.29E+08
	Std	7.553E-06	7.503E-06	0.262911	0.596286	16114.56	2.71E+08	18.677153	215499.71	0.7574214	2.47E+08
F_{14}	Best	0	0	3.65E-80	3.184E-09	4.78E+06	2.69E+07	9292662.1	19252004	7.036E-80	3.78E+08
	Ave	0	3.15E-13	1.55E-79	1.740E-08	10926546	1.03E+08	19227042	42599449	4.336E-69	6.09E+08
	Std	0	5.97E-13	6.42E-80	1.221E-08	2998518	6.25E+07	5145656.3	16751582	7.989E-69	1.62E+08
F_{15}	Best	0	0	1.39E-242	6.959E-51	1.82E+91	1.00E+87	4.01E+48	9.8E+115	3.38E-103	1E+150
	Ave	0	4.99E-22	2.07E-232	1.508E-36	1.1E+105	1.3E+130	7.05E+58	5.6E+134	2.346E-76	2.0E+167
	Std	0	1.38E-21	0	3.029E-36	3.4E+105	3.9E+130	2.08E+59	1.6E+135	4.601E-76	Inf
F_{20}	Best	0	0	7.02E-55	48.012577	1232.3292	340.84209	2532.2144	1130.4518	1392.5935	2207.0720
	Ave	0	5.93E-17	1.22E-47	118.89830	1753.3642	627.04210	4271.2554	1552.4654	1748.1748	2703.4246
	Std	0	9.51E-17	3.64E-47	63.707794	350.21936	157.96121	1568.9721	263.67070	438.87525	250.68542
F_{21}	Best	5.665E-08	3.26E-07	0.2235947	5.6208522	16.104337	118.19971	30.223553	32.900658	0.9377225	202.01800
	Ave	2.223E-06	2.73E-06	0.5525457	6.3960533	29.740545	215.20804	64.435702	46.509961	2.0783121	248.50364
	Std	2.538E-06	3.32E-06	0.2805374	0.4403291	9.1181074	67.873437	25.612469	10.719822	0.7990147	35.678386

TABLE 5. Running results of functions F_{14} - F_{17} .

Function	TGWO	TSGWO	SGWO	GWO	SSA	SCA	PSO	ALO	WOA	MFO
F_{14}	Best	0.9980038	0.9980038	9.98E-01	9.98E-01	0.998004	9.98E-01	0.998004	0.9980038	0.9980038
	Ave	0.9980038	0.9980056	2.77E+00	1.69E+00	1.295028	1.99E+00	4.94E+00	2.2835654	3.7446797
	Std	2.729E-09	5.849E-06	2.977148	1.148984	0.939274	1.045544	2.735905	1.7083279	3.6196920
F_{15}	Best	-10.1532	-10.1532	-1.01E+01	-1.02E+01	-10.1532	-4.603159	-10.1532	-3.862782	-3.862664
	Ave	-10.1513	-10.1513	-1.01E+01	-9.64E+00	-8.14865	-2.28E+00	-2.42E+00	-3.862782	-3.853880
	Std	0.002921	0.004428	0.0671368	1.6114947	3.295489	1.6732426	4.0786647	4.334E-14	0.0167595
F_{16}	Best	-10.4028	-10.4028	-1.04E+01	-10.40249	-10.4029	-5.181506	-10.40294	-10.40294	-10.40180
	Ave	-10.3765	-10.3759	-1.03E+01	-1.04E+01	-7.90301	-3.81E+00	-2.96E+00	-7.679150	-8.528151
	Std	0.082006	0.078698	0.0719013	0.0790012	3.30238	1.4767779	4.0236917	3.4151929	2.8697701
F_{17}	Best	-10.5363	-10.5363	-1.05E+01	-1.05E+01	-10.5364	-5.02E+00	-10.53641	-10.53640	-10.53473
	Ave	-10.5361	-10.4062	-1.05E+01	-1.05E+01	-8.91347	-3.21E+00	-2.82E+00	-6.048479	-6.575206
	Std	0.00025	0.408012	0.0363459	0.0011528	3.421448	1.6401118	3.2734334	3.0513984	3.9749297

Step 4: Update X of using Eq. (16); Update the position X' of each wolf using Eq. (20).

$$X' = \frac{X'_1 + X'_2 + X'_3}{3} \tag{20}$$

Step 5: If $f(X') < f(X)$, then $f(X) = f(X')$, otherwise unchanged. If $f(X) < f(X_\alpha)$, then $f(X_\alpha) = f(X)$.

Step 6: Meet the conditions for stopping the algorithm and output the optimal solution $f(X_\alpha)$, otherwise return to Step 2.

The pseudo-code for the grey wolf optimizer based on the tracking mode and the seeking mode is described as follows.

Random initialization of grey wolf population
Initialize a, A, C, SMP, CDC, SRD and velocity
Set the $X_\alpha, X_\beta, X_\delta$

Calculate the fitness values of wolves

Set the X_α as the best search agent

$l = 1$

While ($l < Max_iter$)

for each wolf

Update the position by Eq. (12) $f(X)$

end for

Compute the fitness of each search agents in the pack

Update the X_1, X_2, X_3 using Eq. (9) - (11)

Update the X using Eq. (12)

for X_1, X_2, X_3

Update X'_1, X'_2, X'_3 by Eq. (16) - (17)

Update X' using Eq. (20)

end for

for every wolf $i = 1, \dots, N$

if $f(X') < f(X)$

$f(X) = f(X')$

end if

end for

if $f(X_\alpha) < f(X)$

$f(X_\alpha) = f(X)$

end if

Update X_α

$l = l + 1$

end while

Output X_α

The flow chart of the grey wolf optimizer based on the tracking mode and the seeking mode is shown in Fig. 5.

IV. SIMULATION EXPERIMENTS AND RESULTS ANALYSIS

A. TEST FUNCTIONS

The numerical efficiency of the improved algorithm developed in this study was tested by solving 21 mathematical optimization problems. Three groups of test functions are employed with different characteristics to test the performance of the improved algorithm from different perspectives: unimodal (F_1 - F_7, F_{18} - F_{19}), multi-modal (F_8 - F_{13}, F_{20} - F_{21}), and fixed-dimension multimodal functions (F_{14} - F_{17}) [58], [59]. The main parameter settings for each algorithm are shown in Table 1. The expressions, dimensions, ranges, and minimum values of the benchmark functions are shown in Table 2. The 3D images of the test functions are shown in Fig. 6.

B. SIMULATIONS AND PERFORMANCE ANALYSIS WITH OTHER ALGORITHMS

The proposed tracking mode based grey wolf optimizer (TGWO), the seeking mode based grey wolf optimizer (SGWO) and the tracking and seeking mode based grey wolf optimizer (TSGWO) were compared with GWO, PSO, SCA, SSA, ALO, WOA and MFO. For each benchmark function, the improved algorithm was run 10 times starting from different populations randomly generated. The average and standard deviation of the best approximated solution in the last iteration are reported in Tables 3-5. The average and standard deviation can compare the overall performance of

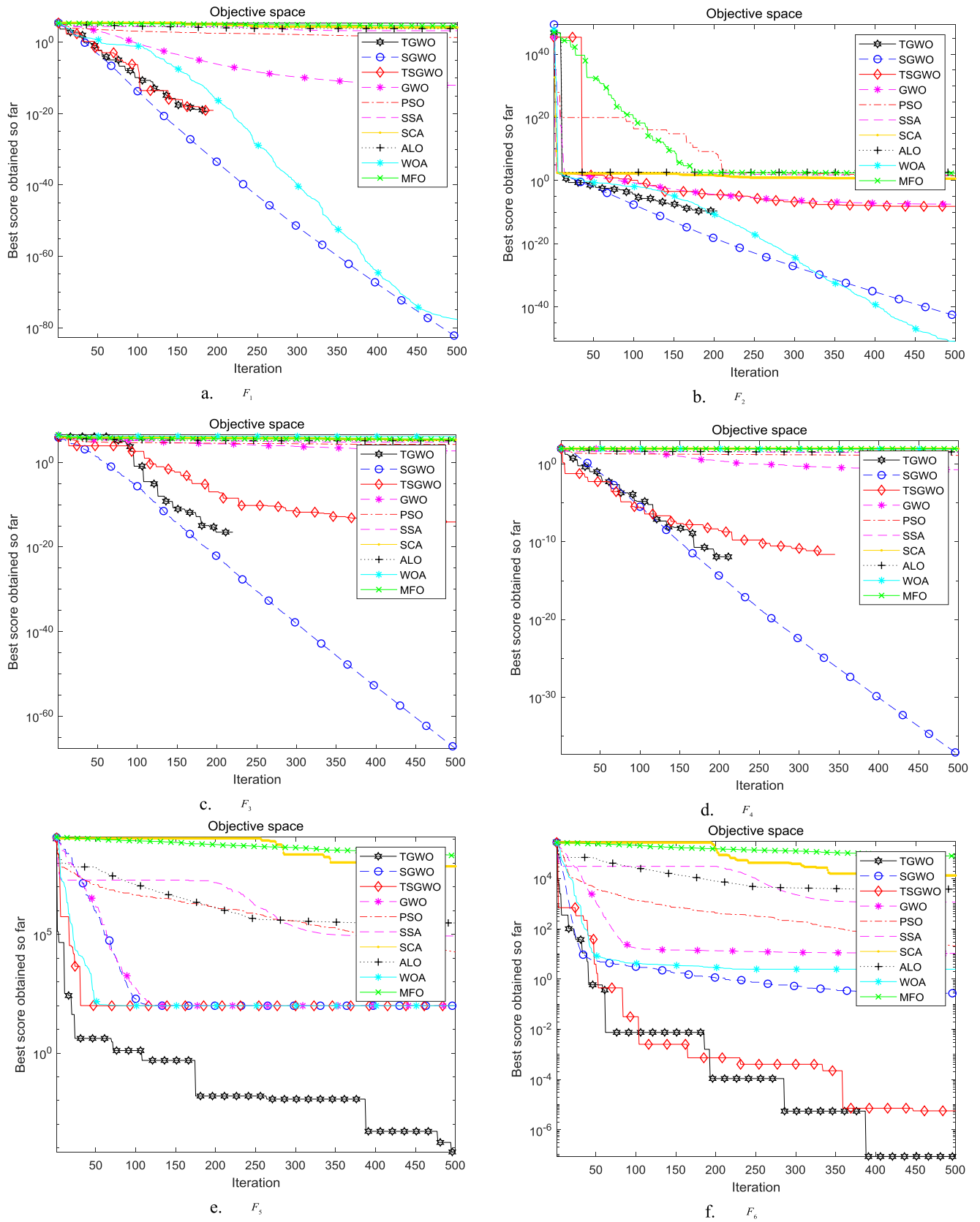


FIGURE 8. Simulation results of function F_1 - F_{13} and F_{18} - F_{21} with 100 dimension.

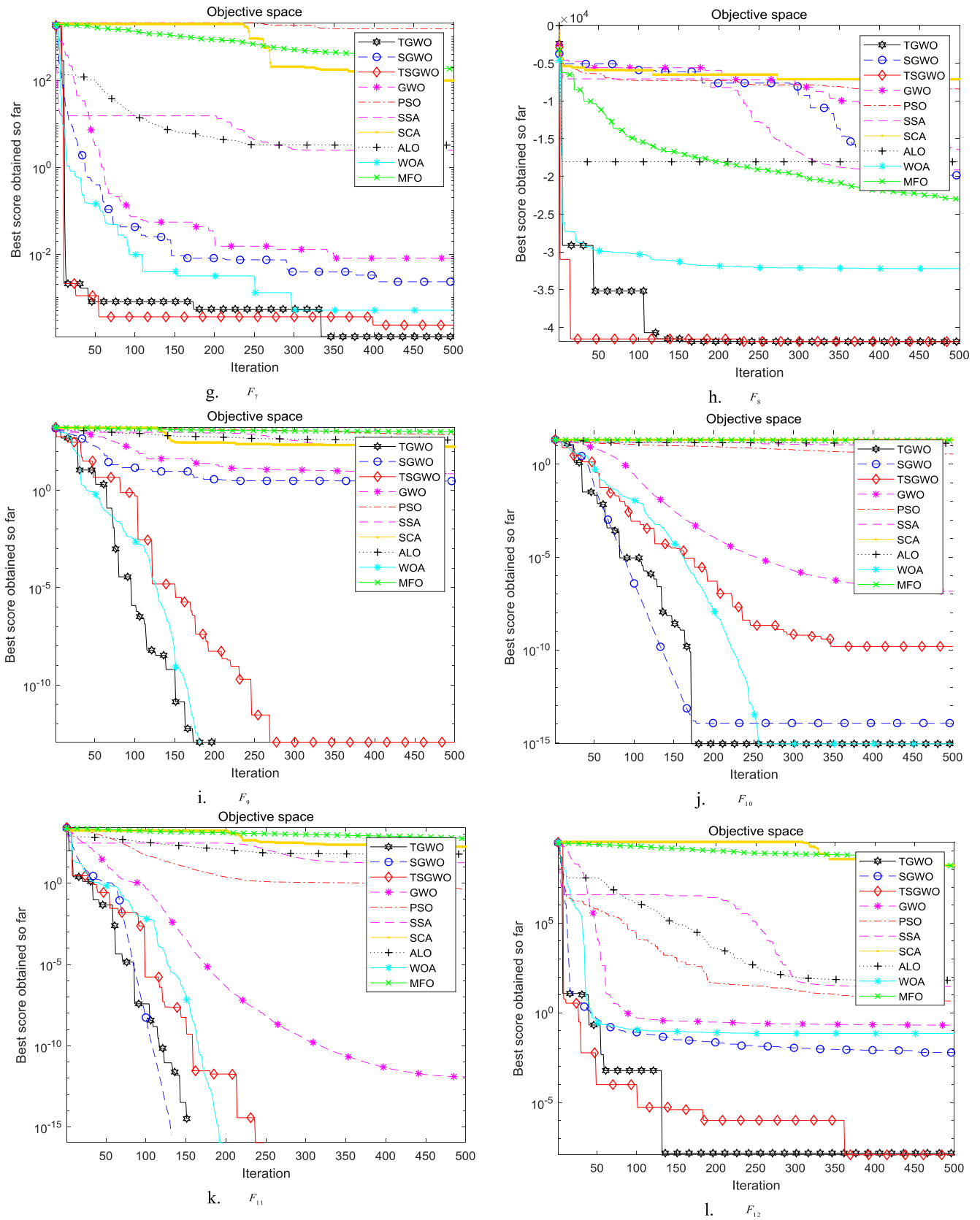


FIGURE 8. (continued.) Simulation results of function F_1 - F_{13} and F_{18} - F_{21} with 100 dimension.

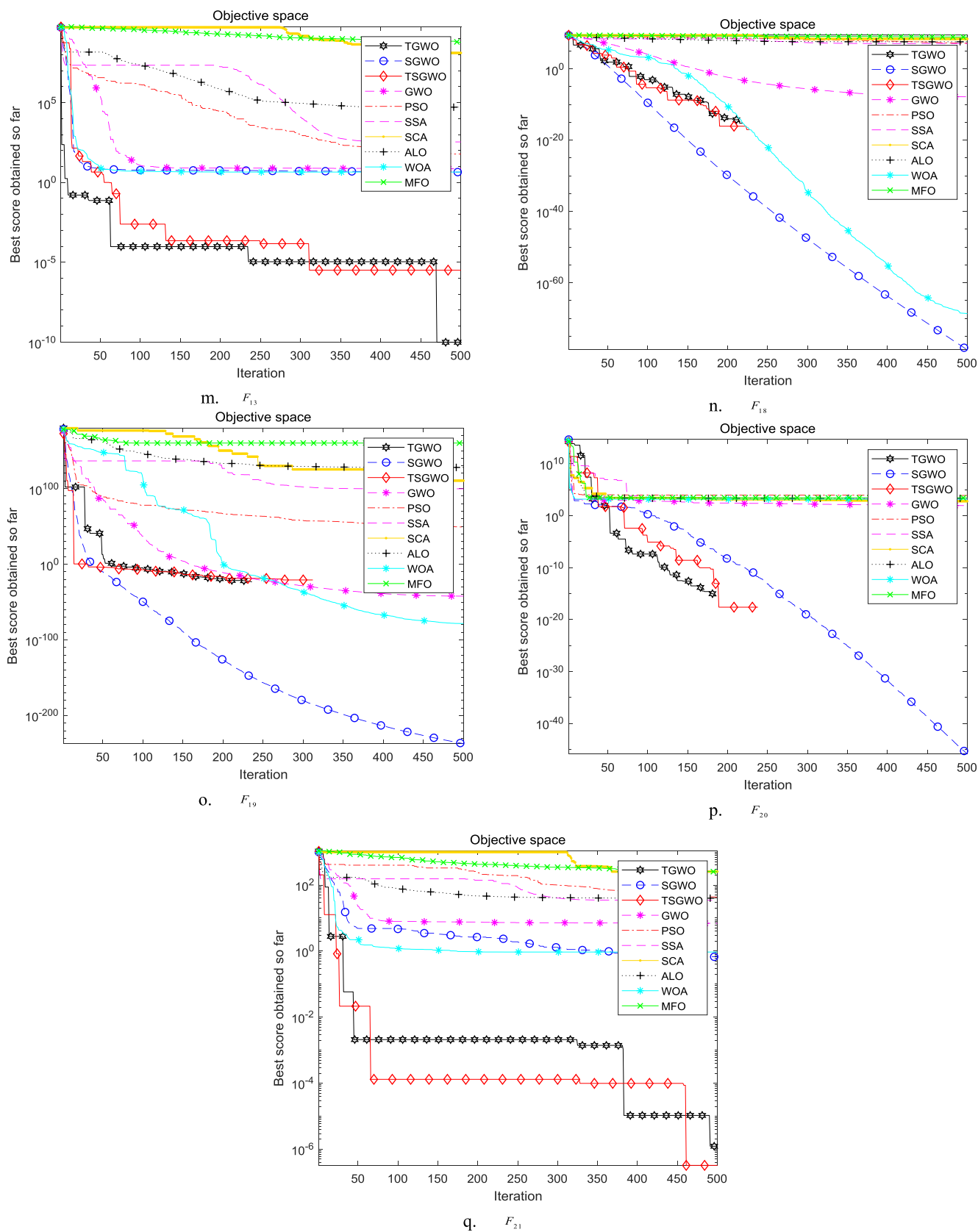


FIGURE 8. (continued.) Simulation results of function F_1 - F_{13} and F_{18} - F_{21} with 100 dimension.

TABLE 6. The improved algorithm optimizes the results of the 30-dimensional function.

Function	TGWO	TSGWO	SGWO	BGWO	PSOGWO	GWOCS	
F_1	Best	0	0	2.79E-100	5	1.88961E-16	3.99731E-30
	Ave	0	1.00E-18	6.60E-99	7	0.049629179	1.47132E-28
	Std	0	3.160E-18	1.171E-98	1.483239697	0.127023545	1.12178E-28
F_2	Best	0	0	6.37E-53	3	2.0732E-09	5.02453E-18
	Ave	0	4.092E-11	1.405E-52	5.6	0.007774751	1.88763E-17
	Std	0	5.215E-11	5.872E-53	1.8	0.015618749	8.89867E-18
F_3	Best	0	0	5.34E-79	185	1.25799E-05	1.57766E-09
	Ave	0	9.13E-09	2.88E-75	502.3	4.608906444	1.40931E-06
	Std	0	2.564E-08	7.51E-75	256.9198513	7.252954603	2.28232E-06
F_4	Best	0	0	1.30E-43	1	3.77393E-05	2.52007E-08
	Ave	0	7.573E-11	6.204E-43	1	0.729861244	2.1322E-07
	Std	0	1.203E-10	6.830E-43	0	1.221175949	1.99851E-07
F_5	Best	2.37E-07	4.49E-06	25.8829	0	25.31980581	26.10097689
	Ave	7.92E-05	1.62E-03	2.74E+01	0	62.12265685	26.74332933
	Std	8.479E-05	0.002978	0.864968	0	102.9002693	0.461726892
F_6	Best	3.117E-09	7.323E-09	0.002881	19.5	0.000481476	7.19782E-05
	Ave	1.599E-06	5.149E-06	0.053341	24.5	159.8841388	0.557912659
	Std	2.065E-06	1.148E-05	0.10519	3	472.565808	0.331016433
F_7	Best	5.690E-07	4.086E-05	0.000475	0.000253305	0.004717094	0.000424824
	Ave	8.692E-05	0.0001210	0.001414	6.600137944	1.068608901	0.002365787
	Std	6.968E-05	7.908E-05	0.000815	5.102896724	2.708482798	0.001791564
F_8	Best	-12569.5	-12569.5	-6735.106	-3155.885543	-7469.99332	-12344.03835
	Ave	-11503.5	-11148.1	-6001.571	-2138.982573	-6624.528358	-10339.23391
	Std	1716.379	1834.979	552.23408	559.1964687	938.6038237	1908.396224
F_9	Best	0	0	0.00E+00	2	17.50227002	1.13687E-13
	Ave	0	1.022E-07	1.50E+00	4.8	115.8175334	6.034148685
	Std	0	3.234E-07	1.956328	1.886796226	115.0012646	4.520819251
F_{10}	Best	8.88E-16	8.881E-16	7.99E-15	1.408535097	8.28345E-10	7.54952E-14
	Ave	8.881E-16	2.467E-11	7.99E-15	1.755853846	3.284355766	9.21929E-14
	Std	6.573E-32	3.587E-11	1.05E-30	0.259866302	4.136470497	1.12403E-14
F_{11}	Best	0	0	0.00E+00	0.166751283	4.75014E-11	0
	Ave	0	0	1.99E-03	0.374193812	0.804843829	0.013210018
	Std	0	0	0.006293	0.129772823	1.059620133	0.011403883
F_{12}	Best	3.355E-10	1.279E-09	9.17E-05	2.271109689	3.91787E-05	0.013827828
	Ave	6.281E-08	2.118E-07	3.39E-03	3.083996788	2.852364277	0.047446508
	Std	8.530E-08	4.813E-07	0.004651	0.510330886	4.737506748	0.029619738
F_{13}	Best	1.007E-08	2.353E-09	5.35E-03	1.34978E-32	0.000564359	0.211372421
	Ave	3.200E-06	2.360E-06	3.01E-01	1.34978E-32	2.06254927	0.685494006
	Std	6.437E-06	2.437E-06	0.172903	2.73691E-48	4.446537626	0.314622226
F_{18}	Best	0	0	9.53E-97	4000001	4.6268E-14	2.18016E-25
	Ave	0	3.922E-16	4.45E-95	6500000.6	0.737248788	1.31177E-24
	Std	0	8.764E-16	5.11E-95	1360147.051	2.185265963	1.29778E-24
F_{19}	Best	0	0	1.30E-249	2	7.35088E-40	2.25068E-90
	Ave	0	1.793E-20	3.44E-242	7.2	1.27944E-05	5.44741E-82
	Std	0	5.204E-20	0	2.441311123	3.65265E-05	1.1497E-81
F_{20}	Best	0	0	2.84E-76	94099.3125	2.71788E-07	7.48432E-11
	Ave	0	4.759E-17	6.86E-74	9828384.45	7.558252449	2.41419E-09
	Std	0	9.517E-17	1.60E-73	16504621.19	20.1593206	1.51874E-09
F_{21}	Best	3.95E-09	2.34E-09	7.06E-03	1.49976E-32	0.536473405	0.903940717
	Ave	3.07E-06	7.49E-06	2.06E-01	1.49976E-32	6.992322825	1.124191417
	Std	3.856E-06	1.513E-05	0.1057708	0	7.913296549	0.141795884

TABLE 7. The improved algorithm optimizes the results of the 100-dimensional function.

Function	TGWO	TSGWO	SGWO	BGWO	PSOGWO	GWOCS	
F_1	Best	0	0	3.61E-84	30	6.73746E-06	1.30389E-13
	Ave	0	6.3799E-19	1.71E-83	37.3	7.394621123	2.43173E-13
	Std	0	1.5090E-18	8.9035E-84	3.1	19.42607375	1.2376E-13
F_3	Best	0	0	7.56E-44	27	0.000762856	8.47777E-09
	Ave	0	3.5470E-10	1.83E-43	33.6	0.217546133	1.60677E-08
	Std	0	4.9404E-10	6.92E-44	3.720215048	0.339386549	5.15434E-09
F_5	Best	0	0	1.10E-69	38722	2047.862647	14.33208648
	Ave	0	6.620789	1.51E-67	43360.6	7152.121285	105.5136212
	Std	0	20.79827	1.92E-67	2993.462751	7268.753252	106.8155241
F_4	Best	0	0	3.72E-38	1	1.893272533	0.021874338
	Ave	0	6.1918E-10	7.45E-38	1	15.76811389	0.041048417
	Std	0	1.4893E-09	4.45E-38	0	8.079216746	0.02662816
F_5	Best	5.28E-08	7.68E-05	9.70E+01	0	96.90472603	95.84690088
	Ave	2.94E+01	19.60225	9.81E+01	0	141.2640239	97.85584126
	Std	47.33739	41.31913	0.489007	0	80.26195064	0.868132965
F_6	Best	3.4897E-08	2.0939E-09	3.49E-03	89	2.634523913	8.253228447
	Ave	1.9794E-06	3.2853E-06	0.416697	97.2	578.4037303	9.638204668
	Std	3.0775E-06	2.8299E-06	0.360974	3.944616585	1704.349276	0.817473379
F_7	Best	1.239E-05	1.2572E-05	2.71E-03	189.0000342	0.042651213	0.002283741
	Ave	7.255E-05	9.0298E-05	0.005387	372.4001785	164.9966173	0.005989512
	Std	7.4631E-05	8.4848E-05	0.002386	104.1548134	317.1606282	0.002165213
F_8	Best	-41898.3	-41898.3	-20042.9941	-5691.493273	-23073.07237	-40633.83537
	Ave	-40713.4	-35976.3	-17378.9666	-4065.909849	-19008.28404	-39327.23192
	Std	3745.167	6242.233	1517.194984	1196.588468	2363.793417	1047.634022
F_9	Best	0	0	0.00E+00	26	166.3720835	1.56888E-11
	Ave	0	0.015555	1.704361	29.9	382.8816321	7.957748514
	Std	0	0.049188	2.370799	2.62488095	223.4891332	6.529549527
F_{10}	Best	8.8817E-16	8.8817E-16	1.51E-14	2.107583099	0.000227698	2.46445E-08
	Ave	3.0393E-13	7.1983E-10	1.51E-14	2.259019836	7.775703249	4.71199E-08
	Std	7.6893E-13	1.5501E-09	0	0.09883011	7.229476725	1.59377E-08
F_{11}	Best	0	0	0.00E+00	0.43951543	2.25948E-06	5.78426E-14
	Ave	0	0	0	0.507559301	5.095451798	0.004785819
	Std	0	0	0	0.04016556	9.328217949	0.009609256
F_{12}	Best	1.5134E-09	4.4986E-10	1.82E-04	2.947206608	0.057114866	0.180396426
	Ave	4.263E-08	6.3383E-08	0.009242	3.414322166	2.884802048	0.257993117
	Std	5.4236E-08	1.2194E-07	0.006104	0.28599502	3.624982625	0.054333808
F_{13}	Best	1.9441E-11	6.4682E-07	3.84E+00	1.34978E-32	6.18778232	5.605733819
	Ave	4.4824E-06	7.1816E-06	4.172949	1.34978E-32	21.61387691	6.671631216
	Std	7.5534E-06	7.5033E-06	0.262911	2.73691E-48	27.40040914	0.514790859
F_{18}	Best	0	0	3.65E-80	3000000	4.1732E-13	2.83609E-26
	Ave	0	3.14717E-13	1.55E-79	6100000.3	6.714019181	1.20438E-24
	Std	0	5.96723E-13	6.42E-80	1920937.099	19.83210843	1.83099E-24
F_{19}	Best	0	0	1.40E-242	4	5.12125E-31	1.6418E-90
	Ave	0	4.98808E-22	2.08E-232	7.3	0.034175483	2.06792E-82
	Std	0	1.37553E-21	0	1.734935157	0.102521563	6.04161E-82
F_{20}	Best	0	0	7.02E-55	23750.3407	3.7378E-07	5.39683E-11
	Ave	0	5.93055E-17	1.22E-47	6215031.09	9.952808369	1.23347E-08
	Std	0	9.50593E-17	3.64E-47	9400066.398	22.34136311	2.15696E-08
F_{21}	Best	5.66523E-08	3.25515E-07	0.223594734	1.49976E-32	0.76339015	0.823589727
	Ave	2.22324E-06	2.72592E-06	0.55254576	1.49976E-32	8.758266648	1.082573416
	Std	2.53823E-06	3.32381E-06	0.280537452	0	8.08317627	0.155778232

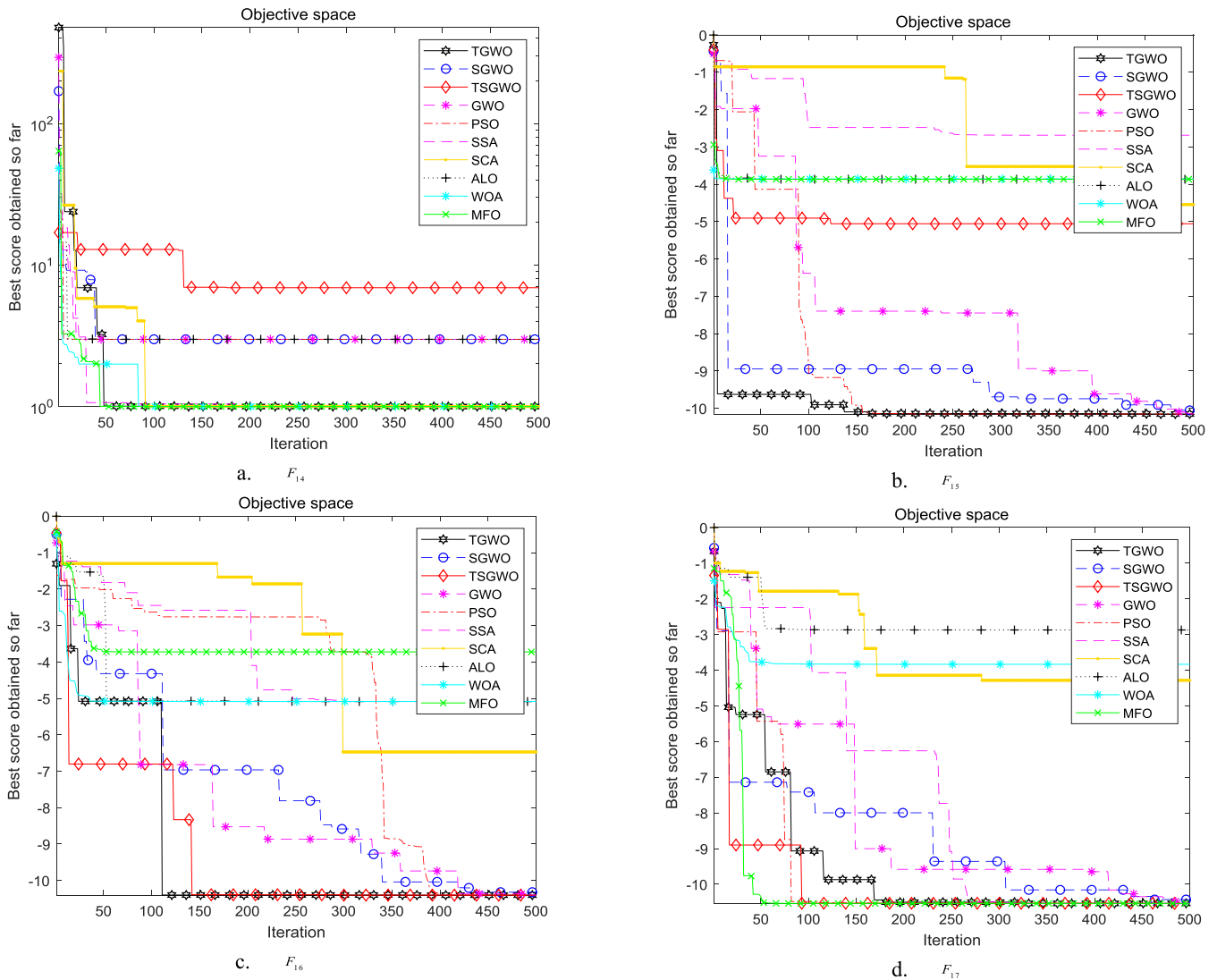


FIGURE 9. Simulation results of function F_{14} - F_{17} .

the algorithm. The convergence curve can intuitively show the optimization performance of the algorithm. The convergence curves of 30-dimensional unimodal and multimodal functions are shown in Fig. 7, and The convergence curves of 100-dimensional unimodal and multimodal functions are shown in Fig. 8. The convergence curves of fixed-dimension multimodal functions are shown in Fig. 9. The simulation results show that the proposed improved algorithms are superior to other algorithms for most test cases of unimodal functions and multimodal functions.

According to the results of the algorithms on the unimodal test functions in Table 3 and the convergence curves of the 30-dimensional unimodal functions, Fig. 7(a)-(g) and Fig. 7(n)-(o), it is evident that the TGWO algorithm outperforms other algorithms on the majority of unimodal benchmark functions, followed by SGWO. TGWO can converge to the

optimal value 0 by optimizing the unimodal functions F_{1-4} and F_{18-19} ; For functions F_5 and F_9 , TGWO has the best optimization effect, followed by TSGWO; The average value of the optimization function F_6 of the SSA algorithm is the closest to the optimal solution and the standard deviation is the smallest. The convergence curves of the 100-dimensional unimodal functions are shown in Fig. 8(a)-(g) and Fig. 8(n)-(o). From results of in Table 4, it can be concluded that the optimal value obtained by TGWO algorithm for optimizing unimodal functions F_{1-4} , F_7 , F_{18} and F_{19} is the closest to the optimal solution; the convergence towards the optimum only in final iterations as may be observed in F_5 and F_6 , but the average value obtained by the TSGWO algorithm is the closest to the optimal value of the function, and its standard deviation is also the smallest.

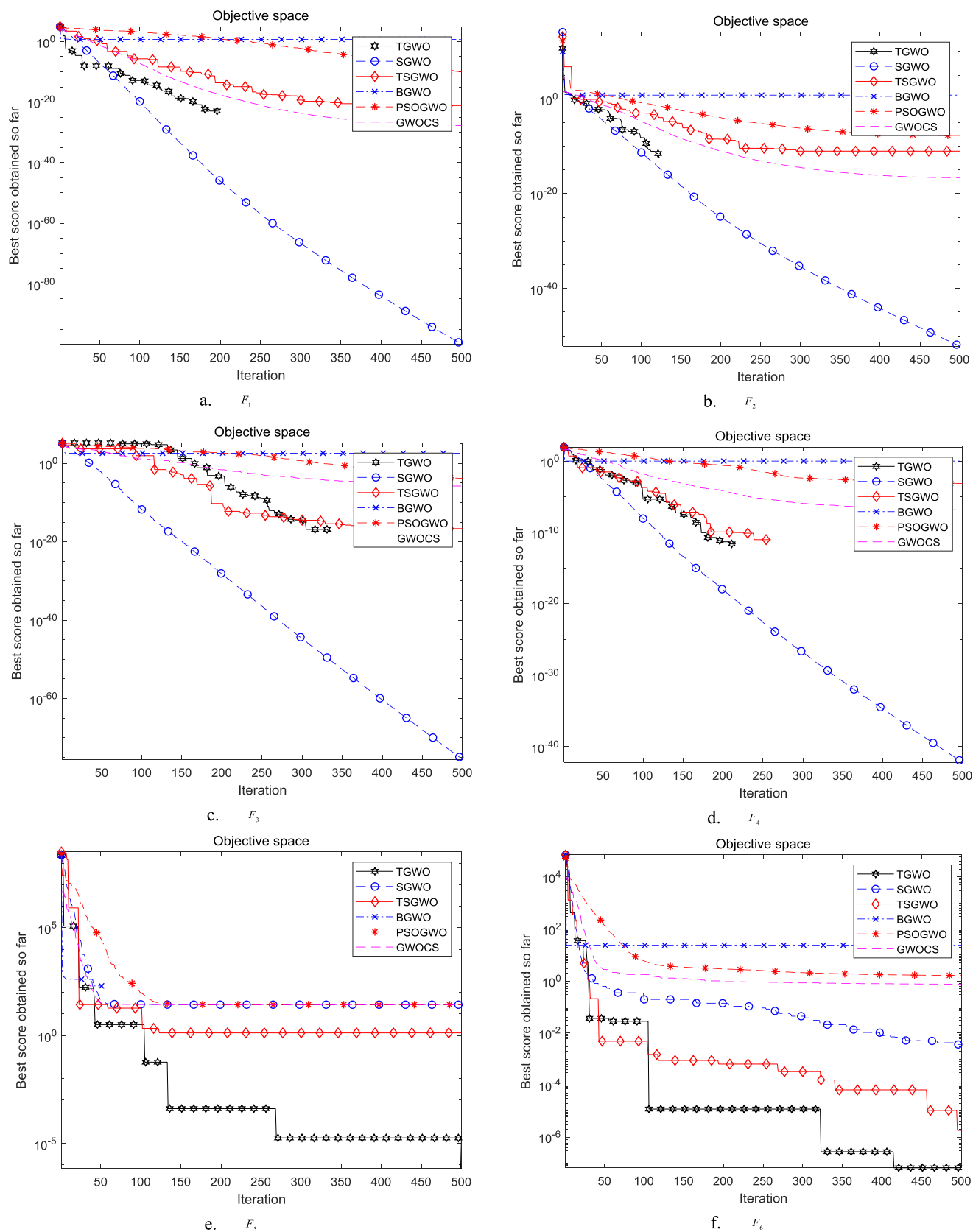


FIGURE 10. Simulation results of function F_1 OF F_{13} and F_{18} - F_{21} with 30 dimension.

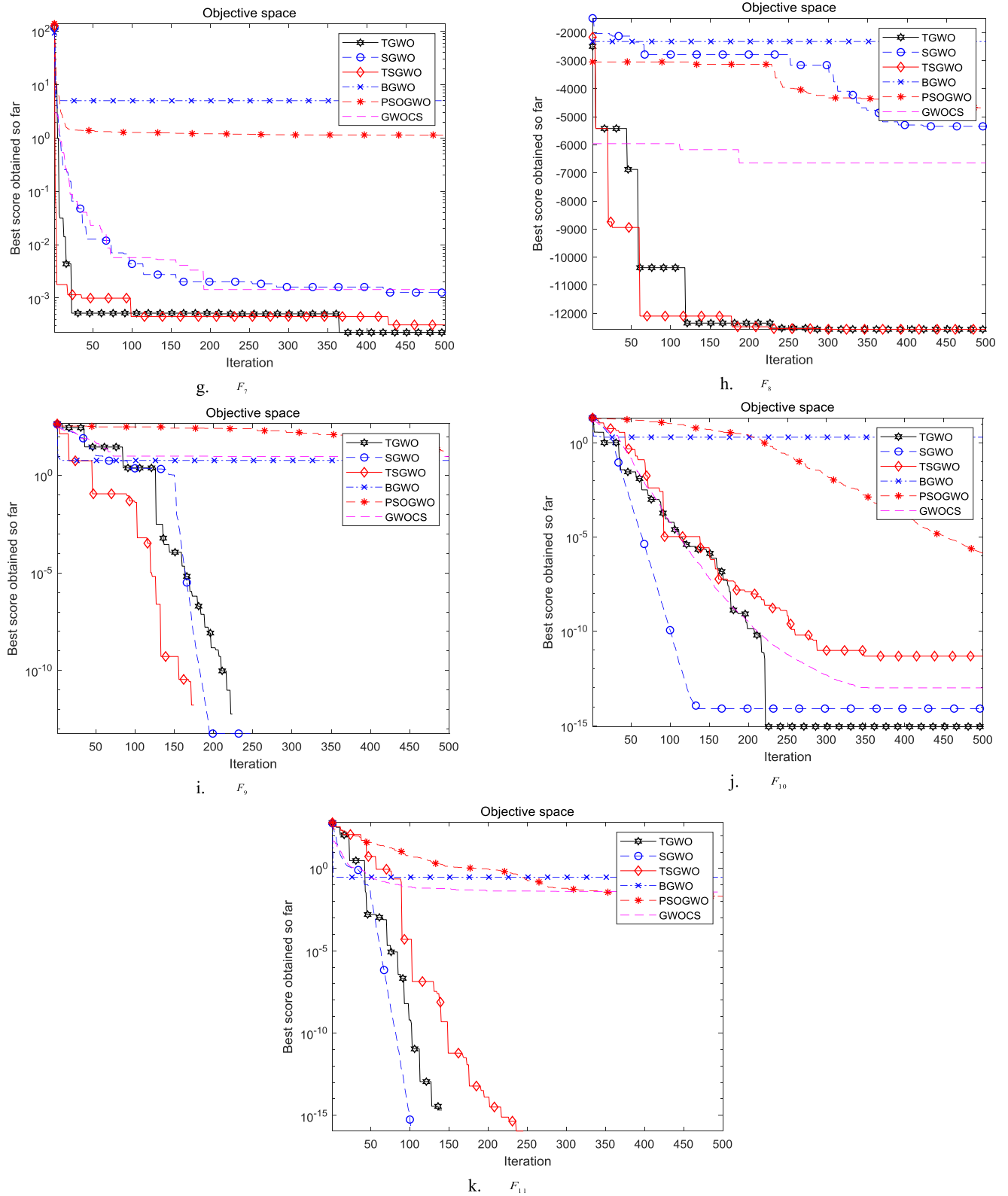


FIGURE 10. (continued.) Simulation results of function F_1 – F_{13} and F_{18} – F_{21} with 30 dimension.

For 30-dimensional multimodal functions, it can be seen from Fig. 7(h)–(m) and Fig. 7(p)–(q). This figure shows that

the TGWO shows the fastest convergence on the composite test functions as well. From the average and standard deviation

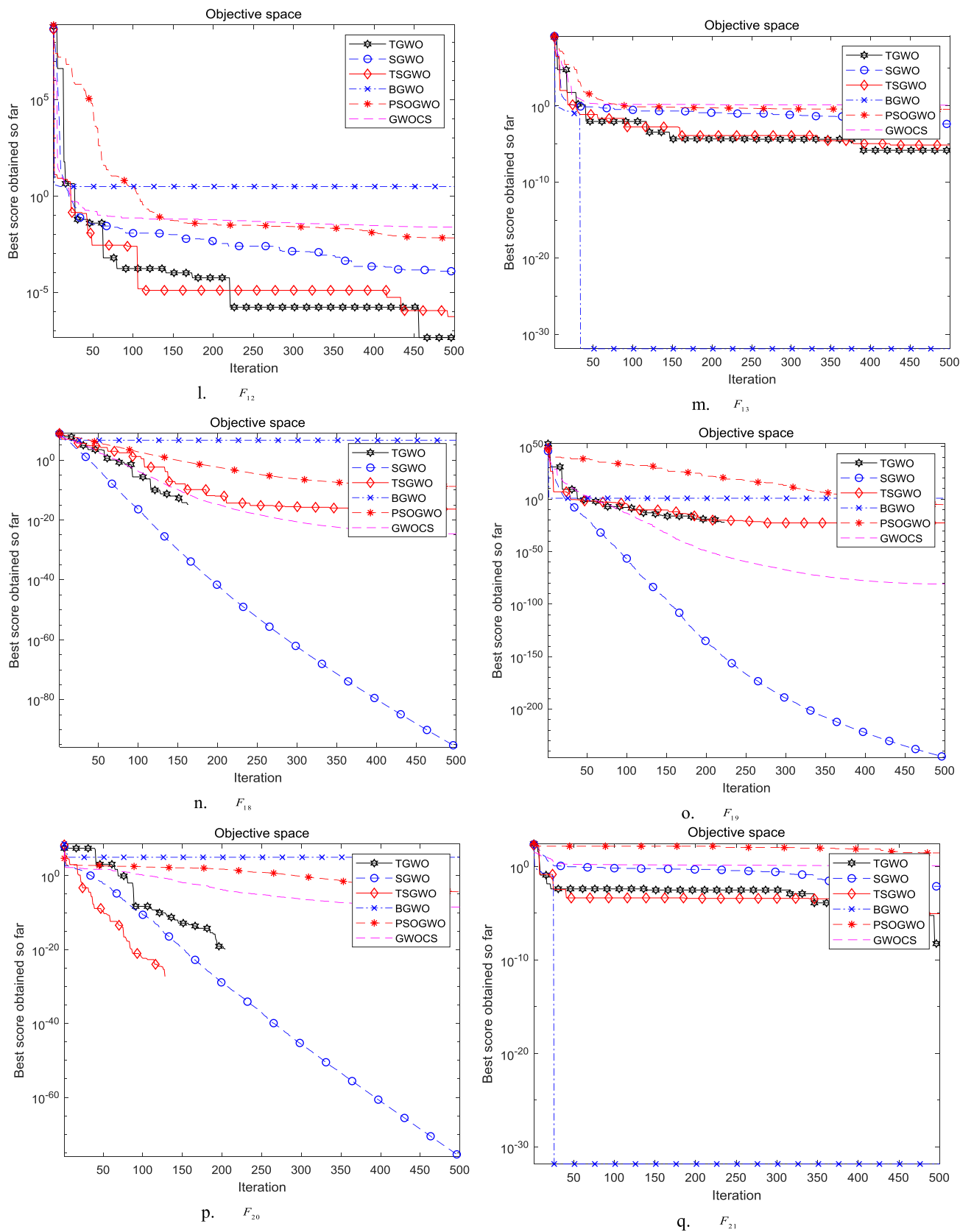


FIGURE 10. (continued.) Simulation results of function F_{10} , F_{13} and F_{18} - F_{21} with 30 dimension.

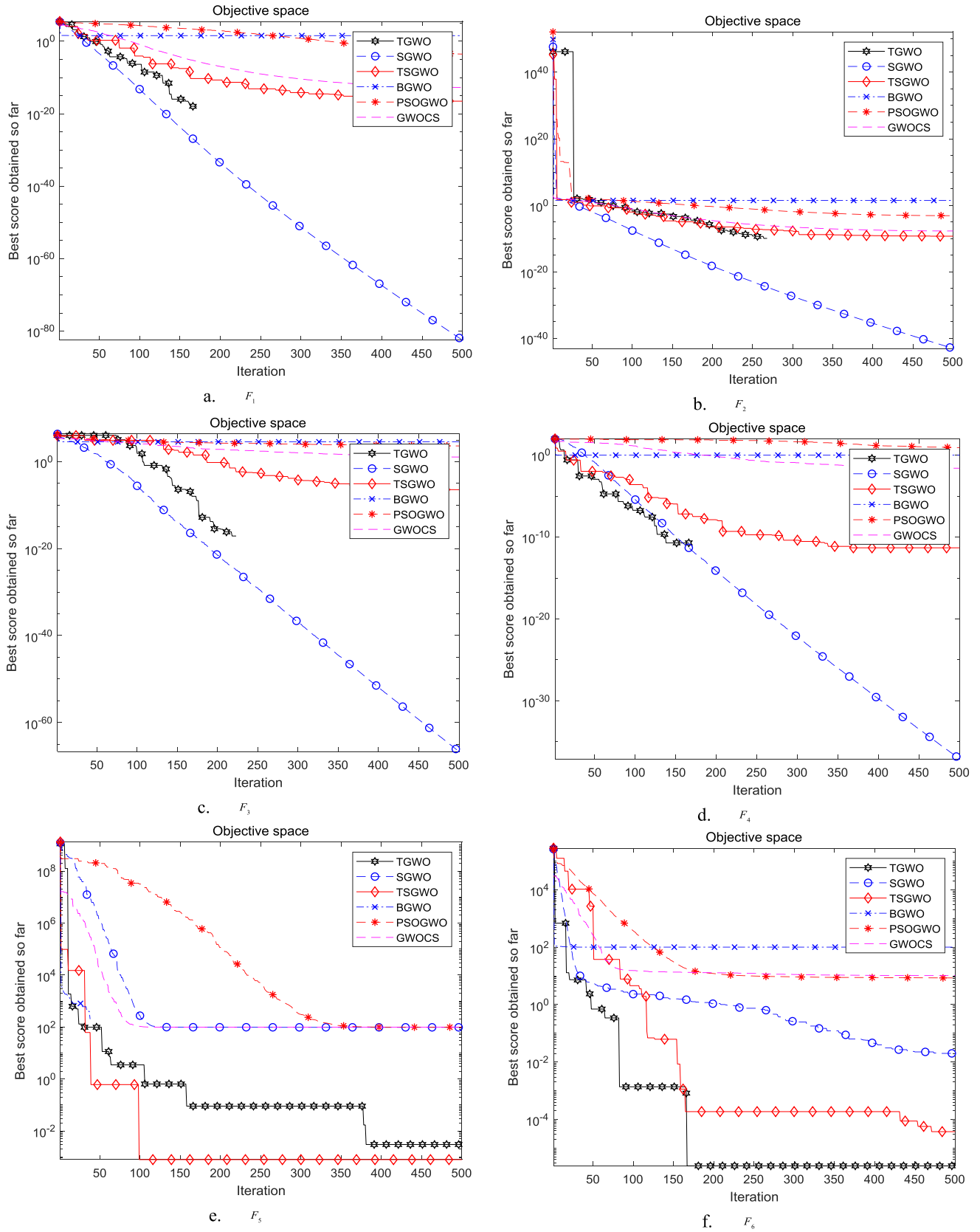


FIGURE 11. (continued.) Simulation results of function F_1 - F_{13} and F_{18} - F_{21} with 100 dimension.

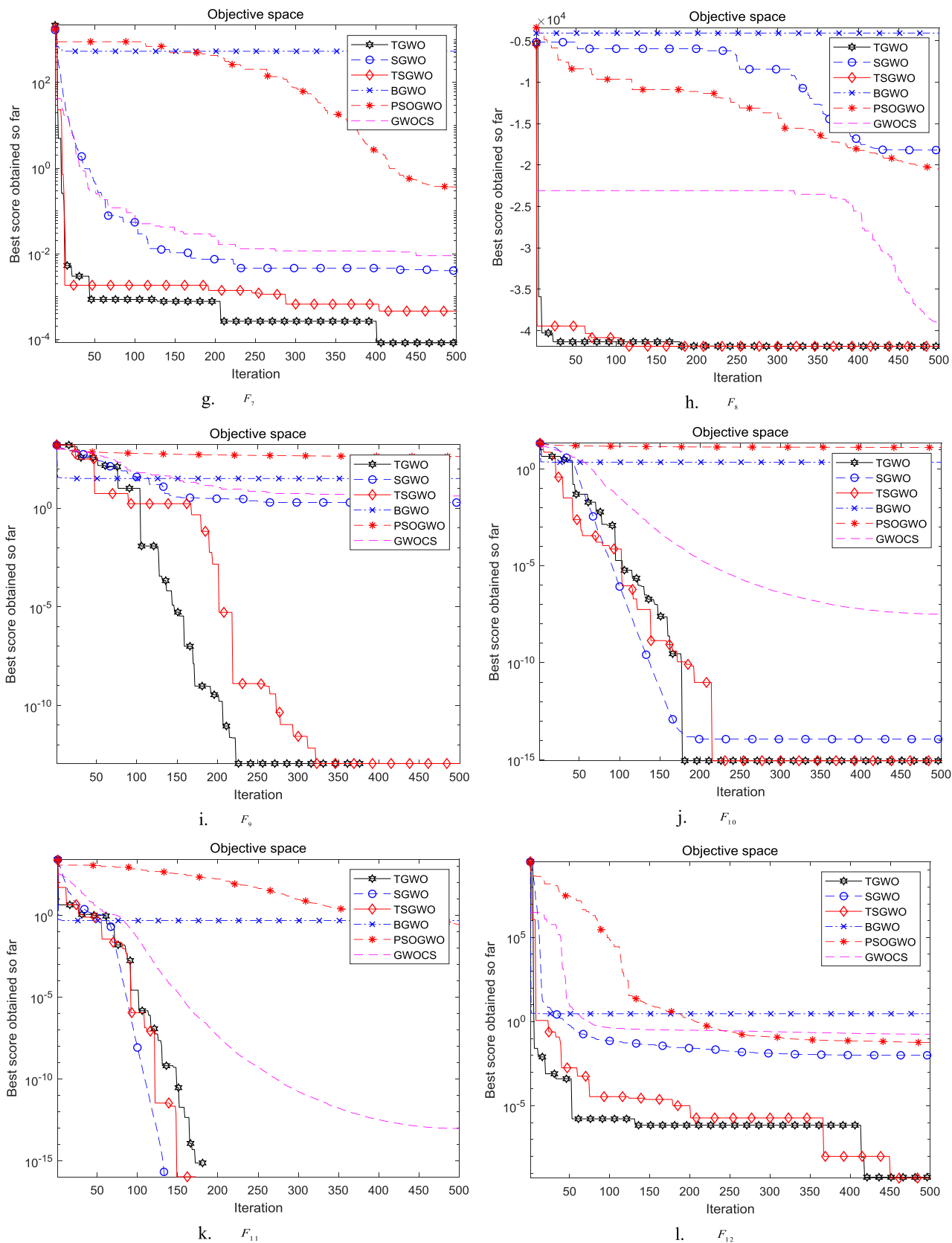


FIGURE 11. (continued.) Simulation results of function F_1 - F_{13} and F_{18} - F_{21} with 100 dimension.

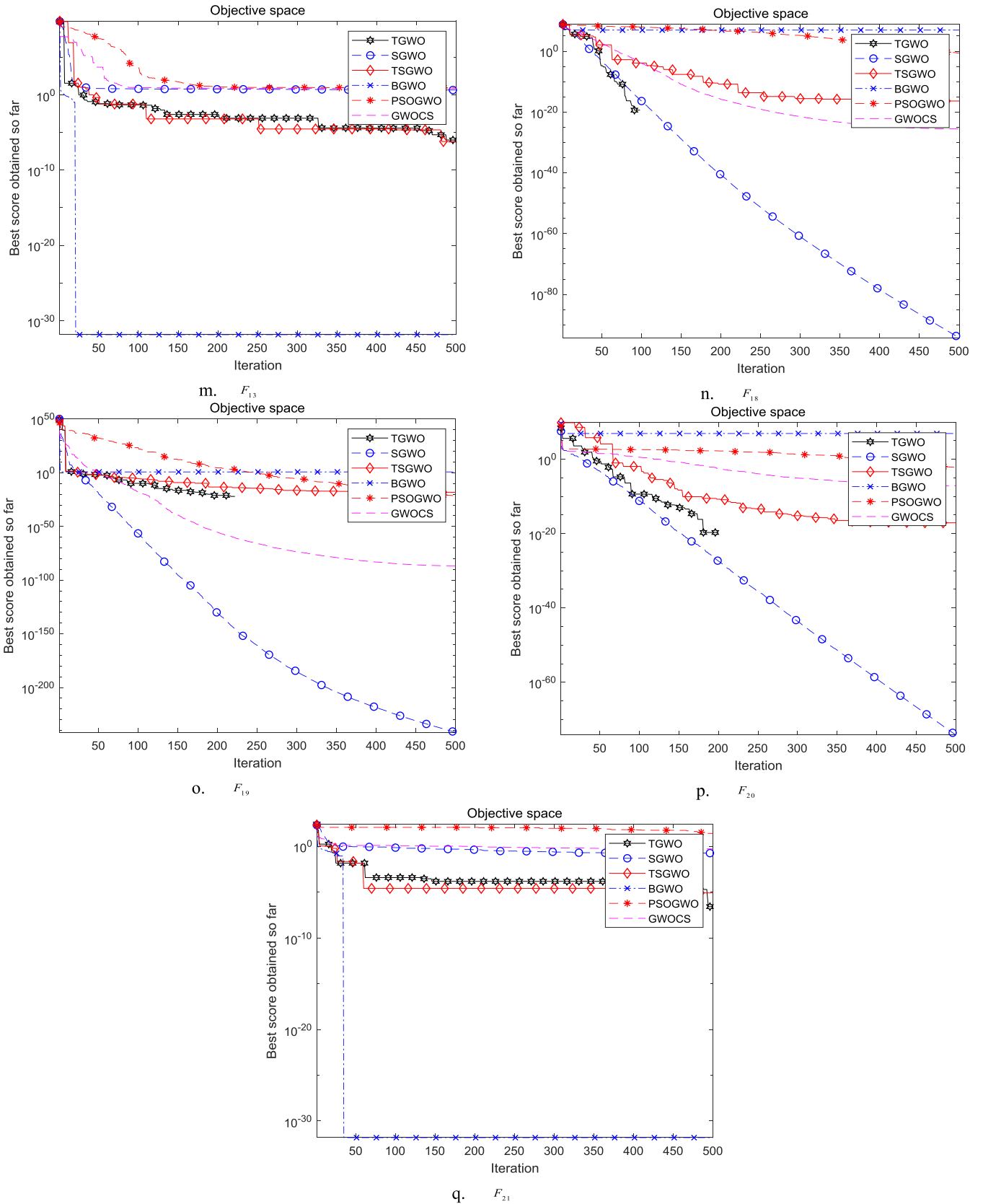


FIGURE 11. (continued.) Simulation results of function F_1 - F_{13} and F_{18} - F_{21} with 100 dimension.

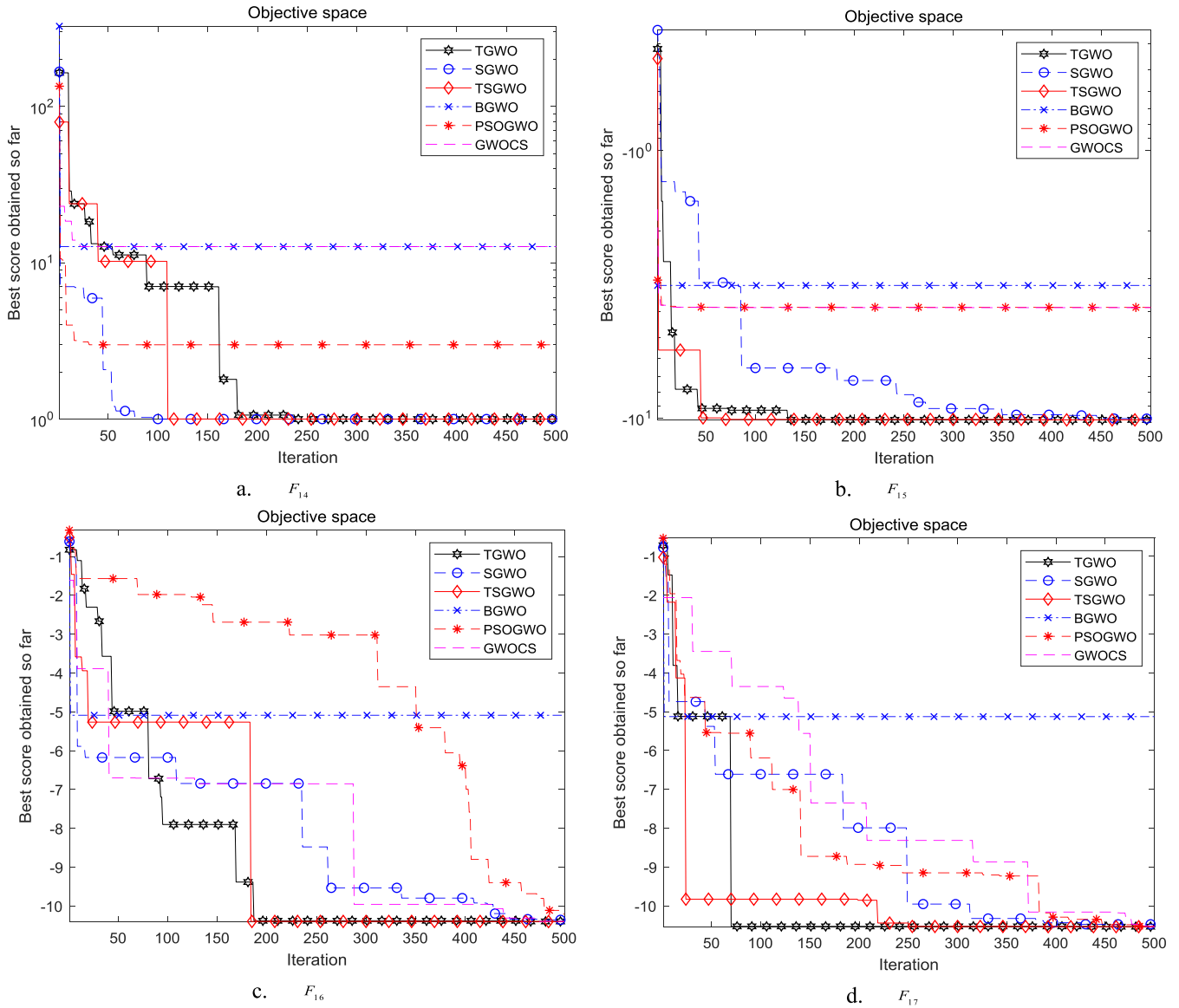


FIGURE 12. Simulation results of function F_{14} - F_{17} .

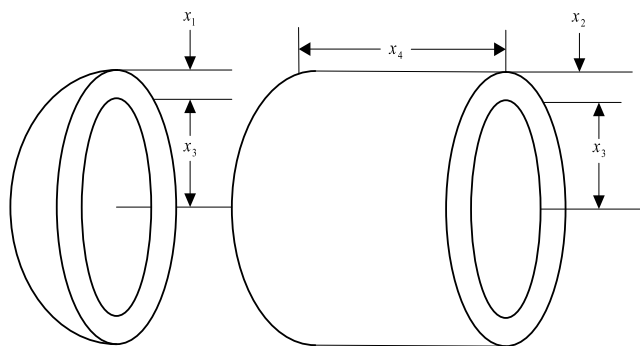


FIGURE 13. Structural diagram of pressure vessel.

tion in Table 3, it can be concluded that the TGWO algorithm is superior to other algorithms in most function optimizations.

The result obtained by the optimization function F_{11} indicate that there are three algorithms that can achieve the optimal value, including TGWO, TSGWO and WOA. The result of optimization function F_{13} of TSGWO algorithm is the best of these algorithms. For the fixed-dimension multimodal functions of F_{14} - F_{17} , The convergence curve of fixed-dimension multimodal functions is shown in Fig. 9(a)-(d), it can be seen from Table 5 that the improved algorithms can obtain the optimal solution. To sum up, the results verify the performance of the improved GWO algorithms in solving various benchmark functions compared to well-known meta-heuristics.

C. SIMULATION EXPERIMENTS AND PERFORMANCE ANALYSIS OF IMPROVED ALGORITHMS

This section compares the improved algorithm with other improved grey wolf optimizer algorithms including Binary

TABLE 8. Improved algorithm optimizes the results of functions F_{14} - F_{17} .

Function		TGWO	TSGWO	SGWO	BGWO	PSOGWO	GWOCs
F_{14}	Best	0.998003838	0.998003838	9.98E-01	12.67050581	0.998003838	0.998003838
	Ave	0.998003839	0.99800569	2.77E+00	12.95493596	1.908235292	4.911929929
	Std	2.72902E-09	5.84957E-06	2.977148	0.434474232	1.78872777	4.353425284
F_{15}	Best	-10.1532	-10.1532	-1.01E+01	-3.761842352	-3.862781107	-3.862778314
	Ave	-10.1513	-10.1513	-1.01E+01	-3.488992552	-3.860772748	-3.862455843
	Std	0.002921	0.004428	0.06713686	0.205679176	0.003047333	0.000741534
F_{16}	Best	-10.4028	-10.4028	-1.04E+01	-5.087666505	-10.40258777	-10.40195538
	Ave	-10.3765	-10.3759	-1.03E+01	-5.087666505	-8.465836669	-9.342167177
	Std	0.082006	0.078698	0.07190131	8.88178E-16	2.930322062	2.117232978
F_{17}	Best	-10.5363	-10.5363	-1.05E+01	-5.12847104	-10.5364025	-10.53571613
	Ave	-10.5361	-10.4062	-1.05E+01	-5.12847104	-8.822871396	-8.91725517
	Std	0.00025	0.408012	0.036345902	0	2.997096053	2.470741477

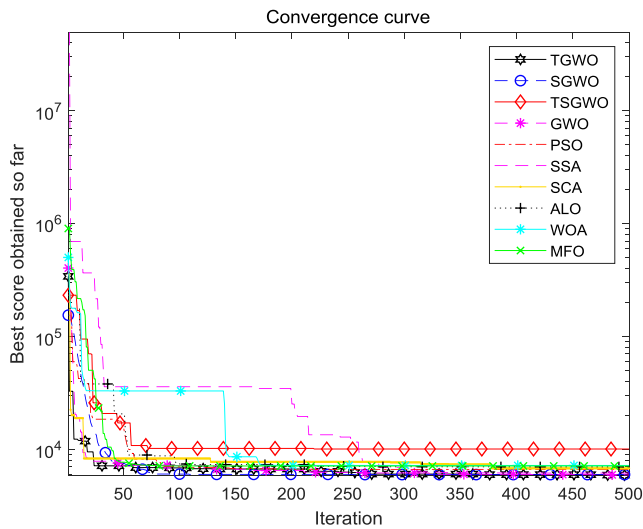


FIGURE 14. Optimal convergence curve of pressure vessel.

Grey Wolf Optimizer (BGWO), Hybrid PSOGWO Optimization (PSOGWO) and GWO Algorithm Integrated with Cuckoo Search (GWOCs). Optimization of 21 functions fully proves the superiority of the algorithm proposed in this paper. To further prove the merits of the proposed improved algorithms, this subsection solves the 30-dimensional and 100-dimensional versions of the unimodal and multimodal test functions. The experimental results are composed of some statistical parameters, such as best, average and standard deviation. Statistical results are reported in Tables 6-8.

The convergence curves of 30-dimensional unimodal multimodal functions are shown in Fig. 10, The convergence curves of the algorithms on some of the 100-dimensional multimodal test functions are illustrated in Fig. 11. It can be seen from Table 6-7 that TGWO is very competitive with other improved algorithms. In particular, it was the most

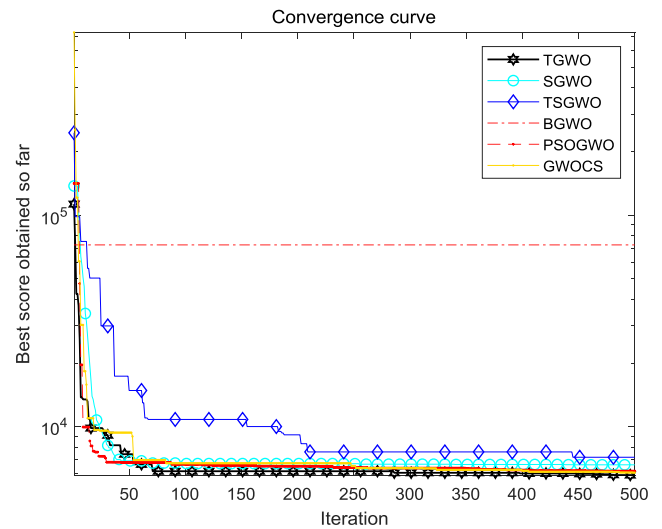


FIGURE 15. The improved algorithm optimizes the convergence curve of pressure vessel.

efficient optimizer for functions F_1 - F_4 , F_8 - F_{12} and F_{20} , and at least the second best optimizer in most test problems. The improved algorithm can hence provide very good exploitation. Another fact that can be seen is the accelerated trend in the convergence curves.

The convergence curves of the TGWO, TSGWO, SGWO, BGWO, PSOGWO and GWOCs are provided in Fig. 12 to see the convergence rate of the algorithms. Tables 8 include the results of fixed-dimension multimodal functions. As the results presented in Table 8, the TGWO algorithm outperforms others in all of the composite test functions. This proves that improved algorithms can well balance exploration and exploitation phases.

As a summary, the results of this section revealed the superiority of the proposed improved algorithm.

TABLE 9. Operation results of pressure vessel optimization.

	TGWO	SGWO	TSGWO	GWO	SSA	SCA	PSO	ALO	WOA	MFO
$f(x)$	5903.0960	5956.6969	8682.2527	5953.6976	6756.4863	6551.4757	6253.5260	6734.9635	7838.9070	5936.103
X_1	0.7819978	0.7842694	1.1387159	0.81413593	0.9397063	0.8559054	0.9518984	1.1095405	1.3722880	0.806804
X_2	0.3879695	0.3887739	0.6085798	0.40220529	0.4644977	0.4218888	0.4705238	0.5484547	0.5853596	0.398803
X_3	40.500745	40.570703	54.401659	42.1552733	48.689440	42.627307	49.321162	57.488976	61.282916	41.80331
X_4	197.71148	198.783657	95.639283	175.982998	126.16258	182.55069	103.82387	48.345247	28.133430	180.3283

TABLE 10. Statistical results of pressure vessel optimization.

	TGWO	SGWO	TSGWO	GWO	SSA	SCA	PSO	ALO	WOA	MFO
Best	5895.8638	5911.6415	7167.5627	5900.3391	6014.6869	6543.7810	6130.2524	5980.6877	6783.9231	5885.3332
Ave	5909.2125	6411.4448	8706.1373	6021.1199	6903.8324	6748.2716	6319.6555	6875.7872	8791.6244	6486.1927
Std	12.550257	385.57122	859.65909	225.62690	670.41450	133.09074	214.13735	1173.4103	1430.4332	640.50406

TABLE 11. Operation results of pressure vessel optimization.

	TGWO	SGWO	TSGWO	BGWO	PSOGWO	GWOCS
$f(x)$	5903.0960	5956.6969	8682.2527	72420.91207	6176.218874	6069.815262
X_1	0.7819978	0.7842694	1.1387159	3.777627474	0.919529633	0.869011589
X_2	0.3879695	0.3887739	0.6085798	3.411969403	0.454876589	0.43111171
X_3	40.500745	40.570703	54.401659	78.64237079	47.64237381	45.00190716
X_4	197.71148	198.783657	95.639283	54.91091476	118.2610832	143.7695802

TABLE 12. Statistical results of pressure vessel optimization.

	TGWO	SGWO	TSGWO	BGWO	PSOGWO	GWOCS
Best	5895.8638	5911.6415	7167.5627	5900.3391	6014.6869	6543.7810
Ave	5909.2125	6411.4448	8706.1373	6021.1199	6903.8324	6748.2716
Std	12.550257	385.57122	859.65909	225.62690	670.41450	133.09074

D. OPTIMAL DESIGN OF PRESSURE VESSELS

The lightest design of pressure vessel is a common optimization problem in practical engineering. Pressure vessel design is to reduce the cost on the premise of safety. The structure of the pressure vessel is shown in Fig. 13.

Objective Function:

$$f(X) = 0.6224X_1X_3X_4 + 1.7781X_2X_3^2 + 3.1661X_1^2X_4 + 19.84X_1^2X_3$$

Constraint Condition:

$$g_1(X) = 0.0193X_3 - X_1 \leq 0$$

$$g_2(X) = 0.00954X_3 - X_2 \leq 0$$

$$g_3(X) = 1296000 - \pi X_3^2X_4 - 4/3\pi X_3^3 \leq 0$$

$$g_4(X) = X_4 - 240 \leq 0$$

where X_1 and X_2 are head (Th) and cylinder wall thickness (Ts), $0.0625 \leq X_1, X_2 \leq 6.1875$; X_3 is the radius of the cylinder and head (R), X_4 is the cylinder length (L), $10 \leq X_3, X_4 \leq 200$. Of the four variables, X_1 and X_2 are uniformly discrete variables with an interval of 0.0625, X_3 and X_4 are continuous variables.

Grey wolf optimizer and the improved grey wolf optimizer based on tracking and seeking modes to solve function optimization problems are used for the optimal design of pressure vessels. The maximum number of iterations is set to 500, the results of 10 times of operation are recorded and the optimal value is obtained. The experimental results are shown in Table 9 and 11, the statistical results of average value and

variance are shown in Table 10 and 12. Convergence curves of improved algorithms TGWO, SGWO, TSGWO, GWO, PSO SSA, SCA, ALO, WOA and MFO for pressure vessel optimization are shown in Fig. 14. The convergence curves obtained by TGWO, SGWO, TSGWO, BGWO, PSOGWO and GWOCS optimized pressure vessels are shown in Fig. 15.

According to the results of the convergence curve and the running data, it can be concluded that the improved grey wolf optimizer based on tracking mode (TGWO) has the best effect on the pressure vessel under the condition of meeting the strength, and the variance also has a good stability performance. The application of the improved algorithm in pressure vessel optimization design shows that the algorithm is also suitable for solving challenging practical engineering problems.

V. CONCLUSION

This study presented an improved grey wolf optimizer based on tracking mode and seeking mode. The performance of the proposed improved algorithm was benchmarked on 19 test functions. The results showed that TGWO was able to provide highly competitive results compared to well-known heuristics such as GWO, PSO, SSA, SCA, ALO, WOA, MFO, BGWO, PSOGWO, GWOCS. The simulation results show that the TGWO achieves the balance between exploration and exploitation, and effectively overcomes the lack of grey wolf optimizer in local search ability. The limitation of the improved algorithm in this paper is that it does not optimize discrete engineering problems. Moreover, the results of pressure vessel engineering design problems show that the TGWO algorithm has high performance to solve real problems with unknown and challenging search spaces as well. For future work, these advantages will be applied to other algorithms, such as ant lion optimizer (ALO) and firefly algorithm (FA), to improve the population diversity, reduce the possibility of falling into the local optimum and improve the ability of the algorithm to balance exploration and exploitation.

REFERENCES

- [1] I. Boussaïd, J. Lepagnot, and P. Siarry, "A survey on optimization meta-heuristics," *Inf. Sci.*, vol. 237, pp. 82–117, Jul. 2013.
- [2] J. H. Holland, *Adaptation in Natural and Artificial Systems*. Ann Arbor, MI, USA: Univ. of Michigan Press, 1975, chs. 1–14, p. 211.
- [3] J. Kennedy and R. Eberhart, "Particle swarm optimization," in *Proc. Int. Conf. Neural Netw. (ICNN)*, 1995, pp. 1942–1948.
- [4] Y. Shi and R. C. Eberhart, "Empirical study of particle swarm optimization," in *Proc. Congr. Evol. Comput. (CEC)*, 2002, pp. 1945–1950.
- [5] J. Sun, B. Feng, and W. Xu, "Particle swarm optimization with particles having quantum behavior," in *Proc. Congr. Evol. Comput.*, 2004, pp. 325–331.
- [6] D. Karaboga, "Artificial bee colony algorithm," *Scholarpedia*, vol. 5, no. 3, p. 6915, 2010.
- [7] D. Karaboga and B. Akay, "A comparative study of artificial bee colony algorithm," *Appl. Math. Comput.*, vol. 214, no. 1, pp. 108–132, Aug. 2009.
- [8] X. S. Yang and S. Deb, "Cuckoo search via Lévy flights," in *Proc. World Congr. Nature Biologically Inspired Comput. (NaBIC)*, 2009, pp. 210–214.
- [9] Y. Li and L. Ma, "New meta-heuristic Cuckoo search algorithm," *Syst. Eng.*, vol. 30, no. 8, pp. 64–69, 2012.
- [10] A. H. Gandomi, X.-S. Yang, and A. H. Alavi, "Cuckoo search algorithm: A metaheuristic approach to solve structural optimization problems," *Eng. Comput.*, vol. 29, no. 1, pp. 17–35, Jan. 2013.
- [11] X.-S. Yang and S. Deb, "Cuckoo search: Recent advances and applications," *Neural Comput. Appl.*, vol. 24, no. 1, pp. 169–174, Jan. 2014.
- [12] S. Mirjalili, "The ant lion optimizer," *Adv. Eng. Softw.*, vol. 83, pp. 80–98, May 2015.
- [13] S. Mirjalili, P. Jangir, and S. Saremi, "Multi-objective ant lion optimizer: A multi-objective optimization algorithm for solving engineering problems," *Int. J. Speech Technol.*, vol. 46, no. 1, pp. 79–95, Jan. 2017.
- [14] S. Mirjalili, "SCA: A sine cosine algorithm for solving optimization problems," *Knowl.-Based Syst.*, vol. 96, pp. 120–133, Mar. 2016.
- [15] M. A. Tawhid and V. Savaani, "Multi-objective sine-cosine algorithm (MO-SCA) for multi-objective engineering design problems," *Neural Comput. Appl.*, vol. 31, no. S2, pp. 915–929, Feb. 2019.
- [16] S. Mirjalili, A. H. Gandomi, S. Z. Mirjalili, S. Saremi, H. Faris, and S. M. Mirjalili, "Salp swarm algorithm: A bio-inspired optimizer for engineering design problems," *Adv. Eng. Softw.*, vol. 114, pp. 163–191, Dec. 2017.
- [17] S. Mirjalili and A. Lewis, "The whale optimization algorithm," *Adv. Eng. Softw.*, vol. 95, pp. 51–67, May 2016.
- [18] E. Emary, H. M. Zawbaa, and M. Sharawi, "Impact of Lévy flight on modern meta-heuristic optimizers," *Appl. Soft Comput. J.*, vol. 75, pp. 775–789, Feb. 2018.
- [19] S. Mirjalili, "Moth-flame optimization algorithm: A novel nature-inspired heuristic paradigm," *Knowl.-Based Syst.*, vol. 89, pp. 228–249, Nov. 2015.
- [20] S. H. S. Moosavi and V. K. Bardsiri, "Poor and rich optimization algorithm: A new human-based and multi populations algorithm," *Eng. Appl. Artif. Intell.*, vol. 86, pp. 165–181, Nov. 2019.
- [21] C. E. Klein and S. C. L. Dos, "Meerkats-inspired algorithm for global optimization problems," in *Proc. Eur. Symp. Artif. Neural Netw., Comput. Intell. Mach. Learn.*, 2018, pp. 679–684.
- [22] N. S. Jaddi, J. Alvankarian, and S. Abdullah, "Kidney-inspired algorithm for optimization problems," *Commun. Nonlinear Sci. Numer. Simul.*, vol. 42, pp. 358–369, Jan. 2017.
- [23] S. Shadravan, H. R. Naji, and V. K. Bardsiri, "The sailfish optimizer: A novel nature-inspired metaheuristic algorithm for solving constrained engineering optimization problems," *Eng. Appl. Artif. Intell.*, vol. 80, pp. 20–34, Apr. 2019.
- [24] A. Cheraghali, M. Hajiaghaei-Keshteli, and M. M. Paydar, "Tree growth algorithm (TGA): A novel approach for solving optimization problems," *Eng. Appl. Artif. Intell.*, vol. 72, pp. 393–414, Jun. 2018.
- [25] M. Jain, V. Singh, and A. Rani, "A novel nature-inspired algorithm for optimization: Squirrel search algorithm," *Swarm Evol. Comput.*, vol. 44, pp. 148–175, Feb. 2019.
- [26] G. G. Wang, S. Deb, and L. D. S. Coelho, "Earthworm optimisation algorithm: A bio-inspired Metaheuristic algorithm for global optimisation problems," *Int. J. Bio-Inspired Comput.*, vol. 12, no. 1, p. 1, 2018.
- [27] H. P. Williams, "Integer and combinatorial optimization," *J. Oper. Res. Soc.*, vol. 41, no. 2, pp. 177–178, 1990.
- [28] G. Zhu and S. Kwong, "Gbest-guided artificial bee colony algorithm for numerical function optimization," *Appl. Math. Comput.*, vol. 217, no. 7, pp. 3166–3173, Dec. 2010.
- [29] K. Harada, J. Sakuma, I. Ono, and S. Kobayashi, "Constraint-handling method for multi-objective function optimization: Pareto descent repair operator," in *Proc. 4th Int. Conf. Evol. Multi-Criterion Optim. (EMO)*. Matsushima, Japan: Springer-Verlag, Mar. 2007, pp. 156–170.
- [30] A. Verbart, M. Langelaar, and F. V. Keulen, "Damage approach: A new method for topology optimization with local stress constraints," *Struct. Multidisciplinary Optim.*, vol. 53, no. 5, pp. 1081–1098, May 2016.
- [31] F. H. F. Leung, H. K. Lam, S. H. Ling, and P. K. S. Tam, "Tuning of the structure and parameters of a neural network using an improved genetic algorithm," *IEEE Trans. Neural Netw.*, vol. 14, no. 1, pp. 79–88, Jan. 2003.
- [32] K. V. Bury, "Bayesian decision method applied to a problem in gear train design," *Int. J. Prod. Res.*, vol. 9, no. 3, pp. 377–392, Jan. 1971.
- [33] S. Mirjalili, S. M. Mirjalili, and A. Lewis, "Grey wolf optimizer," *Adv. Eng. Softw.*, vol. 69, pp. 46–61, Mar. 2014.
- [34] S. Mirjalili, S. Saremi, S. M. Mirjalili, and L. D. S. Coelho, "Multi-objective grey wolf optimizer: A novel algorithm for multi-criterion optimization," *Expert Syst. Appl.*, vol. 47, pp. 106–119, Apr. 2016.
- [35] H. Xu, X. Liu, and J. Su, "An improved grey wolf optimizer algorithm integrated with Cuckoo search," in *Proc. 9th IEEE Int. Conf. Intell. Data Acquisition Adv. Comput. Syst., Technol. Appl. (IDAACS)*, Sep. 2017, pp. 490–493.

- [36] Z. Teng, J. Lv, L. Guo, and X. Yuanyuan, "An improved hybrid grey wolf optimization algorithm based on Tent mapping," *J. Harbin Inst. Technol.*, vol. 50, no. 11, pp. 46–55, 2018.
- [37] H. Xu, Y. Fu, and X. Liu, "Applying improved grey wolf optimizer algorithm integrated with Cuckoo search to feature selection for network intrusion detection," *Eng. Sci. Technol.*, vol. 50, no. 5, pp. 164–170, 2018.
- [38] J.-S. Wang and S.-X. Li, "An improved grey wolf optimizer based on differential evolution and elimination mechanism," *Sci. Rep.*, vol. 9, no. 1, pp. 1–21, Dec. 2019.
- [39] W. Long, X. Liang, S. Cai, J. Jiao, and W. Zhang, "A modified augmented Lagrangian with improved grey wolf optimization to constrained optimization problems," *Neural Comput. Appl.*, vol. 28, no. S1, pp. 421–438, Dec. 2017.
- [40] M. Kohli and S. Arora, "Chaotic grey wolf optimization algorithm for constrained optimization problems," *J. Comput. Des. Eng.*, vol. 5, no. 4, pp. 458–472, Oct. 2018.
- [41] M. M. Majeed and S. R. Patri, "An enhanced grey wolf optimization algorithm with improved exploration ability for analog circuit design automation," *TURKISH J. Electr. Eng. Comput. Sci.*, vol. 26, no. 5, pp. 2605–2617, 2018.
- [42] E. Emary, H. M. Zawbaa, and C. Grosan, "Experienced gray wolf optimization through reinforcement learning and neural networks," *IEEE Trans. Neural Netw. Learn. Syst.*, vol. 29, no. 3, pp. 681–694, Mar. 2018.
- [43] H. M. Zawbaa, E. Emary, C. Grosan, and V. Snasel, "Large-dimensionality small-instance set feature selection: A hybrid bio-inspired heuristic approach," *Swarm Evol. Comput.*, vol. 42, pp. 29–42, Oct. 2018.
- [44] E. Emary, H. M. Zawbaa, and A. E. Hassanien, "Binary grey wolf optimization approaches for feature selection," *Neurocomputing*, vol. 172, pp. 371–381, Jan. 2016.
- [45] H. M. Zawbaa, J. Szłęk, C. Grosan, R. Jachowicz, and A. Mendyk, "Computational intelligence modeling of the macromolecules release from PLGA microspheres-focus on feature selection," *PLoS ONE*, vol. 11, no. 6, 0, Art. no. e0157610.
- [46] H. M. Zawbaa, S. Schiano, L. Perez-Gandarillas, C. Grosan, A. Michrafy, and C.-Y. Wu, "Computational intelligence modelling of pharmaceutical tableting processes using bio-inspired optimization algorithms," *Adv. Powder Technol.*, vol. 29, no. 12, pp. 2966–2977, Dec. 2018.
- [47] E. Emary and H. M. Zawbaa, "Impact of chaos functions on modern swarm optimizers," *PLoS ONE*, vol. 11, no. 7, 2016, Art. no. e0158738.
- [48] E. Emary, H. M. Zawbaa, and C. Grosan, "Feature subset selection approach by gray-wolf optimization," in *Proc. Afro-Eur. Conf. Ind. Adv. Cham, Switzerland: Springer*, 2015, pp. 1–13.
- [49] S. Gupta and K. Deep, "A novel random walk grey wolf optimizer," *Swarm Evol. Comput.*, vol. 44, pp. 101–112, Feb. 2019.
- [50] A. Saxena, R. Kumar, and S. Das, " β -chaotic map enabled grey wolf optimizer," *Appl. Soft Comput.*, vol. 75, pp. 84–105, Feb. 2019.
- [51] S.-C. Chu, P.-W. Tsai, and J.-S. Pan, "Cat swarm optimization," in *Proc. Pacific Rim Int. Conf. Artif. Intell.*, vol. 6, 2006, pp. 854–858.
- [52] S. D. Yang, Y. L. Yi, and Y. P. Lu, "Homotopy-inspired cat swarm algorithm for global optimization," *Adv. Mater. Res.*, vols. 602–604, pp. 1793–1797, Dec. 2012.
- [53] P.-W. Tsai, J.-S. Pan, S.-M. Chen, B.-Y. Liao, and S.-P. Hao, "Parallel cat swarm optimization," in *Proc. Int. Conf. Mach. Learn. Cybern.*, vol. 6, Jul. 2008, pp. 3328–3333.
- [54] Y. Sharafi, M. A. Khanesar, and M. Teshnehlab, "Discrete binary cat swarm optimization algorithm," in *Proc. 3rd IEEE Int. Conf. Comput., Control Commun. (IC)*, Sep. 2013, pp. 1–6.
- [55] G. Panda, P. M. Pradhan, and B. Majhi, "IIR system identification using cat swarm optimization," *Expert Syst. Appl.*, vol. 38, no. 10, pp. 12671–12683, Sep. 2011.
- [56] L. Guo, Z. Meng, Y. Sun, and L. Wang, "Parameter identification and sensitivity analysis of solar cell models with cat swarm optimization algorithm," *Energy Convers. Manage.*, vol. 108, pp. 520–528, Jan. 2016.
- [57] J. Liu and S. Liu, "An improved dual grey wolf optimization algorithm for unit commitment problem," in *Proc. Int. Conf. Life Syst. Modeling Simulation Int. Conf. Intell. Comput. Sustain. Energy Environ.*, 2017, pp. 156–163.
- [58] J. J. Liang, P. N. Suganthan, and K. Deb, "Novel composition test functions for numerical global optimization," in *Proc. IEEE Swarm Intell. Symp. (SIS)*, Jun. 2005, pp. 68–75.
- [59] N. H. Awad, M. Z. Ali, and P. N. Suganthan, "Ensemble sinusoidal differential covariance matrix adaptation with Euclidean neighborhood for solving CEC2017 benchmark problems," in *Proc. IEEE Congr. Evol. Comput. (CEC)*, Jun. 2017, pp. 372–379.



M. W. GUO is currently pursuing the master's degree with the School of Electronic and Information Engineering, University of Science and Technology Liaoning, Anshan, China.



J. S. WANG (Member, IEEE) received the B.Sc. and M.Sc. degrees in control science from the University of Science and Technology Liaoning, China, in 1999 and 2002, respectively, and the Ph.D. degree in control science from the Dalian University of Technology, China, in 2006. He is currently a Professor and a Master's Supervisor with the School of Electronic and Information Engineering, University of Science and Technology Liaoning. His main research interests include modeling of complex industry process, intelligent control, and computer integrated manufacturing.



L. F. ZHU is currently pursuing the master's degree with the School of Electronic and Information Engineering, University of Science and Technology Liaoning, Anshan, China.



S. S. GUO is currently pursuing the master's degree with the School of Electronic and Information Engineering, University of Science and Technology Liaoning, Anshan, China.



W. XIE is currently pursuing the master's degree with the School of Electronic and Information Engineering, University of Science and Technology at Liaoning, Anshan, China.

...